
# Nanotube Water

*Alexander Kolesnikov*
*IPNS, ANL, Argonne, IL*

Office of Science
U.S. Department of Energy

*A U.S. Department of Energy*
*Office of Science Laboratory*
*Operated by The University of Chicago*

***C.-K. Loong, N. De Souza and P. Thiyagarajan – IPNS, ANL, Argonne, IL***

***J.-M. Zanotti – LLB, Saclay, France***

***C.J. Burnham – Dep. Physics, The University of Houston, Texas***

***A.P. Moravsky and R.O. Loutfy – MER Corporation, Tucson, AZ***

1. ***Introduction***
2. ***Can water enter the SWNT (inner diameter 14 Å)?***
3. ***What are the effects of nanotube confinement on the dynamics of water?***
4. ***MD simulations and proposed nanotube-water structure.***

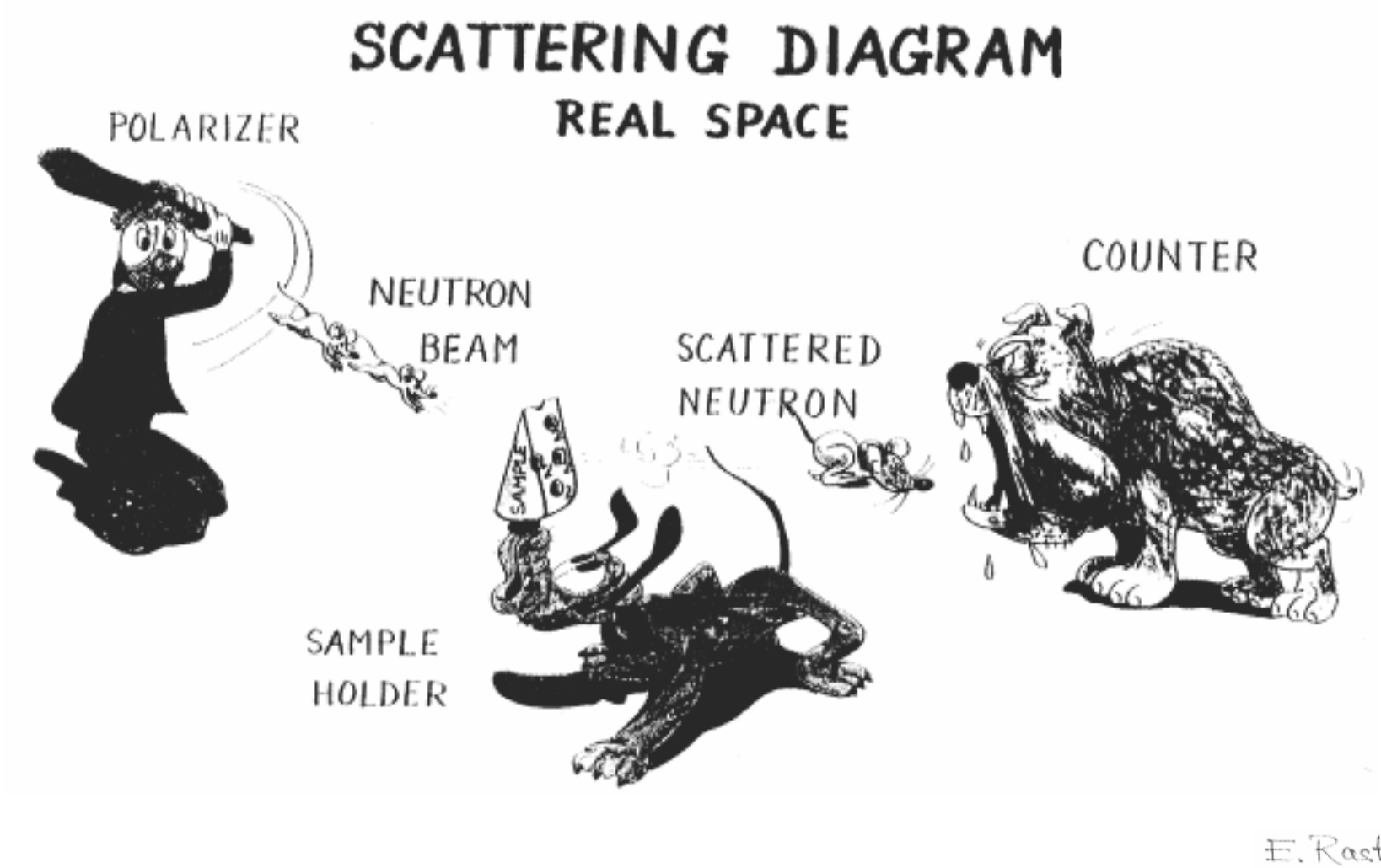
SCATTERING DIAGRAM
REAL SPACE
POLARIZER
NEUTRON
BEAM
SCATTERED
NEUTRON
COUNTER
SAMPLE
HOLDER
SAMPLE
E. Rastelli

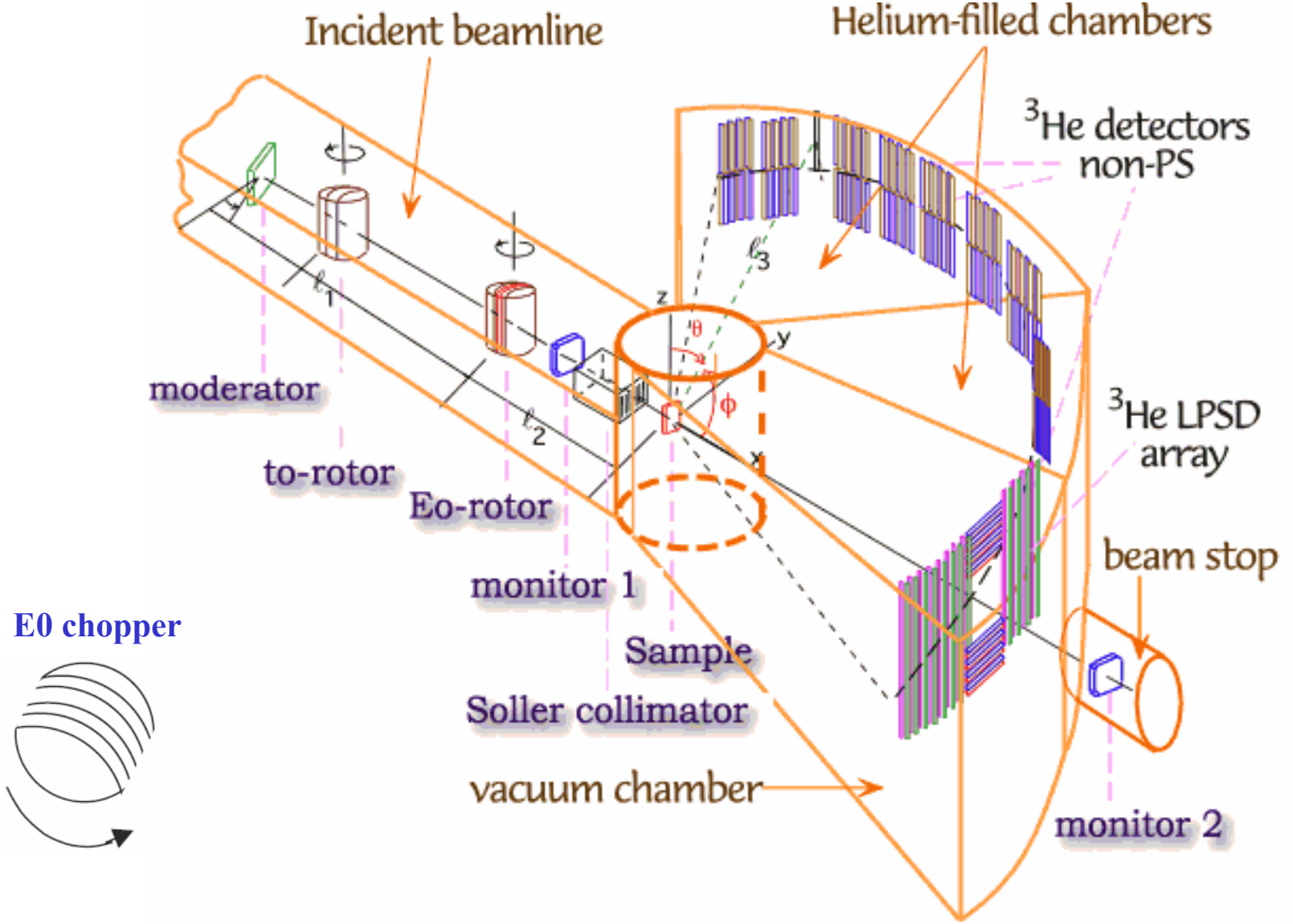


**Direct geometry time-of-flight spectrometer HRMECS at IPNS (ANL).**

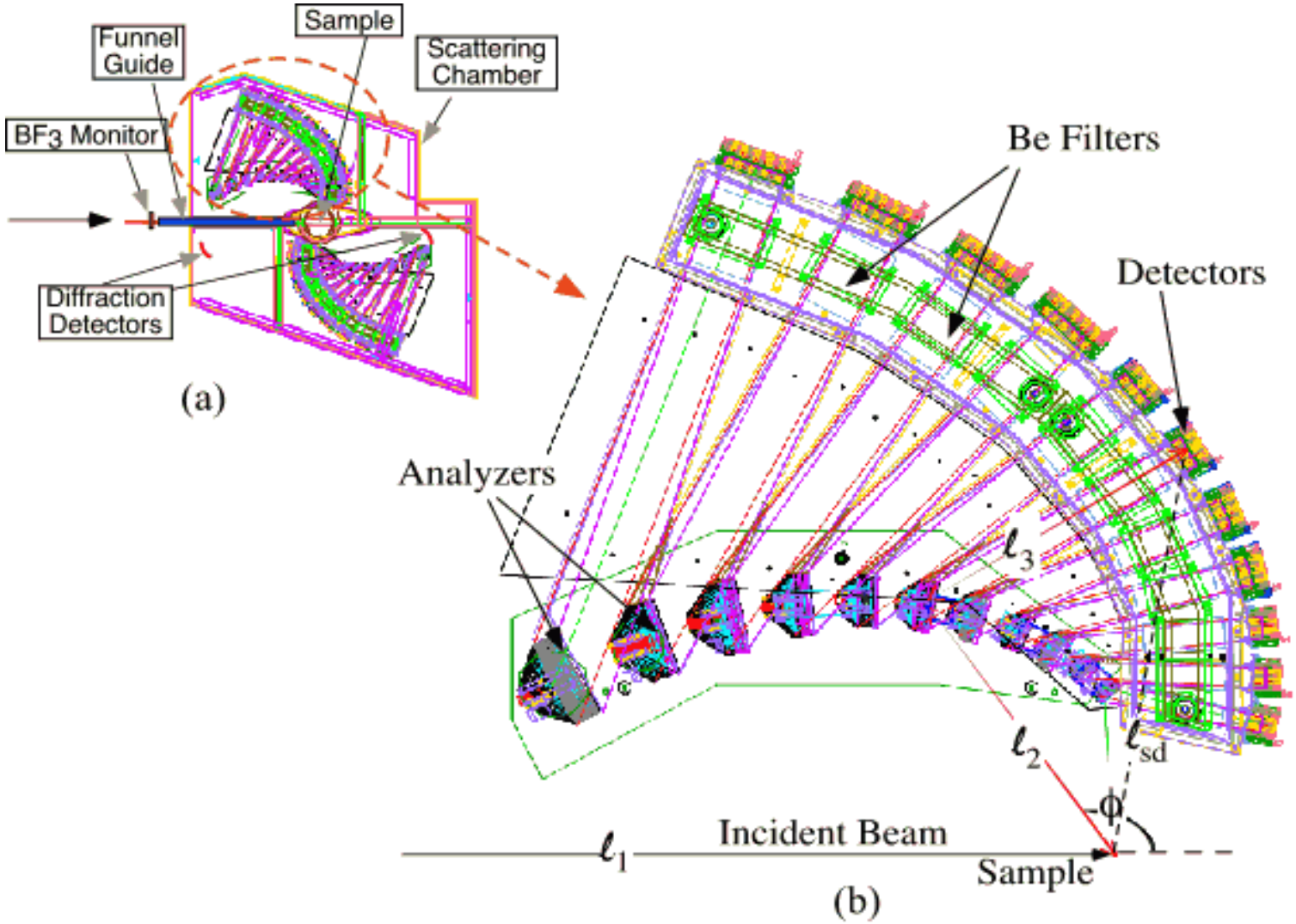


**Inverse geometry time-of-flight spectrometer QENS at IPNS (ANL).**

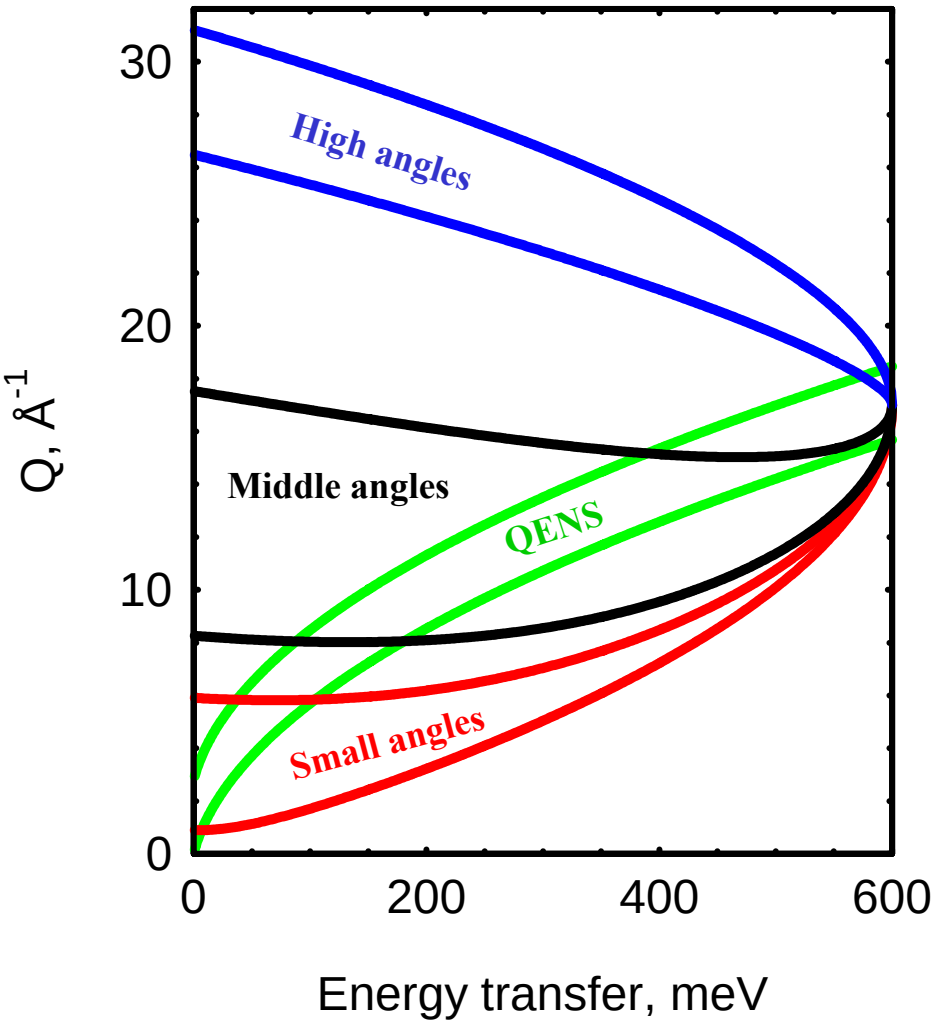


| | Energy Transfer | Q-range Å$^{-1}$ | E-Resolution (FWHM) |
|---|---|---|---|
| **QENS** | Quasi-elastic | 0.3-2.5 | 80 μeV |
| | 0–200 meV | 0.1–30 | 4-5% of E-transfer |
| **HRMECS** | 0–600 meV | 0.1–30 | 2-4% of E-incident |

Comparison of the dynamic range and energy resolution of Quasi-Elastic Neutron Scattering (**QENS**) and High Resolution Medium Energy Chopper Spectrometer (**HRMECS**).

Q dependencies as a function of energy transfer for **QENS** (green curves, angles 0 and 180 degrees) and **HRMECS** (Ei=600 meV, scattering angles: 3-20, 28-62, and 102-133 degrees) spectrometers.

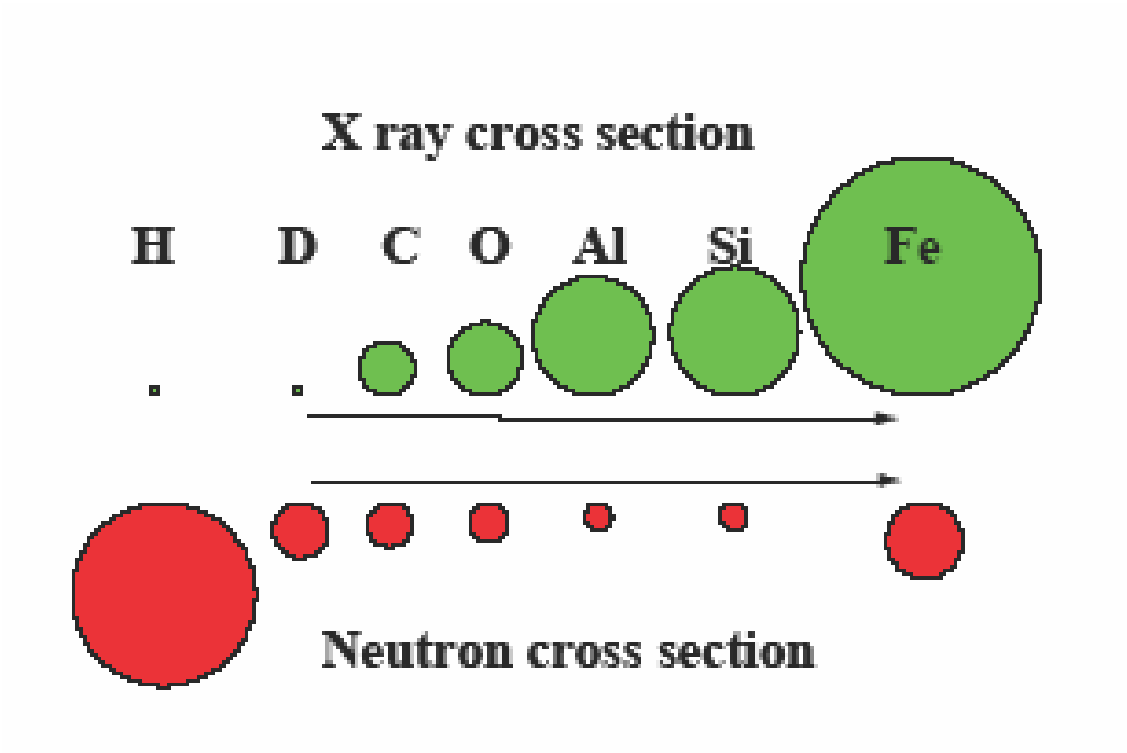
X ray cross section
H
D
C
O
Al
Si
Fe
Neutron cross section

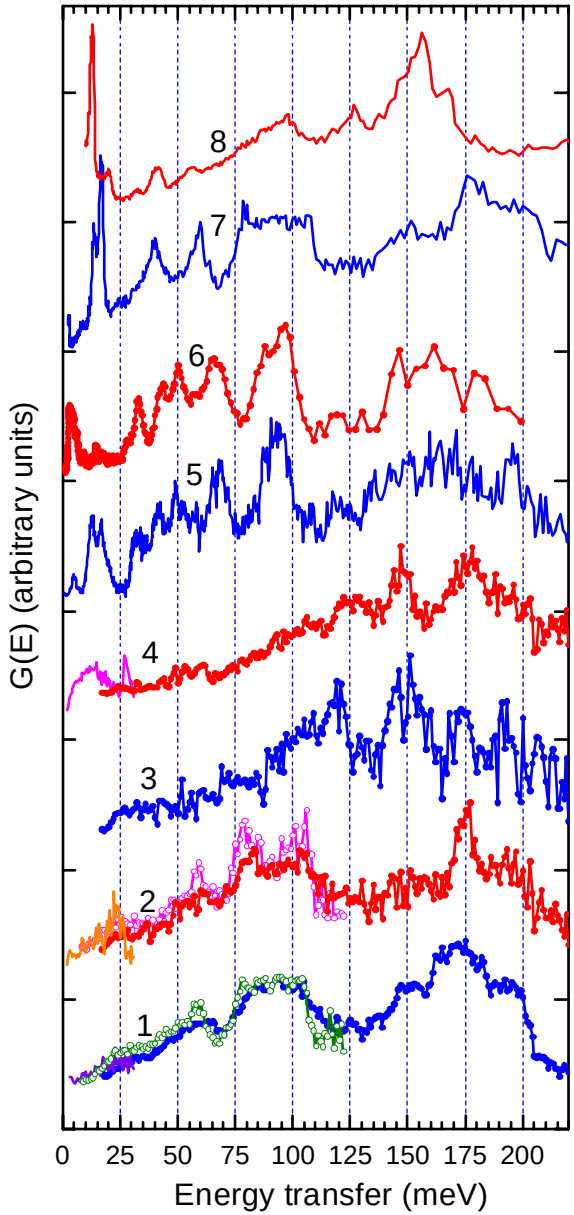


**Generalized vibrational density of sates obtained from INS spectra for different carbon nano-materials:**

**1 – SWNH**
**2 – SWNT**
**3 – DWNT**
**4 – $C_{60}$-peapods**
**5 - high-pressure polymerized $C_{60}$**
**6 - pristine $C_{60}$**
**7 – graphite**
**8 – diamond**

**The spectra 1 to 4 were measured at T=8 K on the direct-geometry HRMECS spectrometer (IPNS, ANL, current work) with different incident neutron energies, $E_i$=280 meV (1-4); 140 meV (1 and 2) and 50 meV (1, 2 and 4). The spectra for pristine and polymerized $C_{60}$ [1], and graphite and diamond ([2], the data have been taken from TFXA database) are shown for comparison.**

**[1] A.I. Kolesnikov *et al., J. Phys.: Cond. Matt.* 8, 10939 (1996).**
**[2] J.K. Walters *et al., J. Phys.: Cond. Matt.* 7, 10059 (1995).**

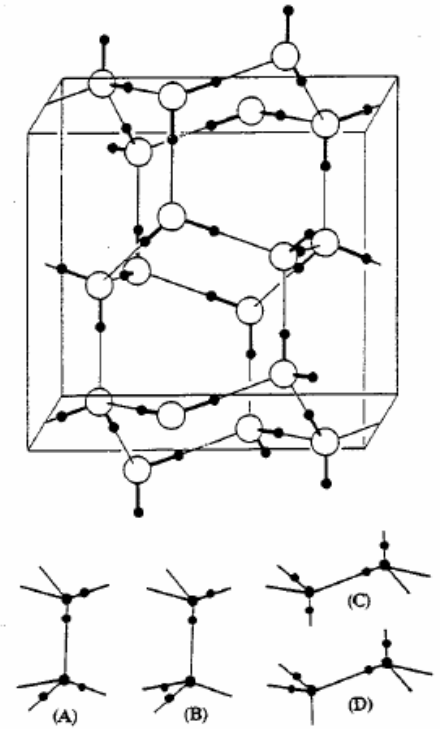


FIG. 1. Schematic structure of ice Ih (space group $P6_3/mmc$): (O) are oxygen positions and (·) are the possible hydrogen positions and four possible orientations of molecule pairs in ice Ih.

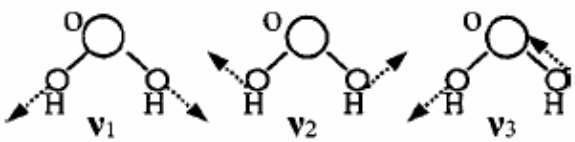


Schematic illustration of the bending, ν2 , and stretching, ν1 and ν3, modes in water molecule

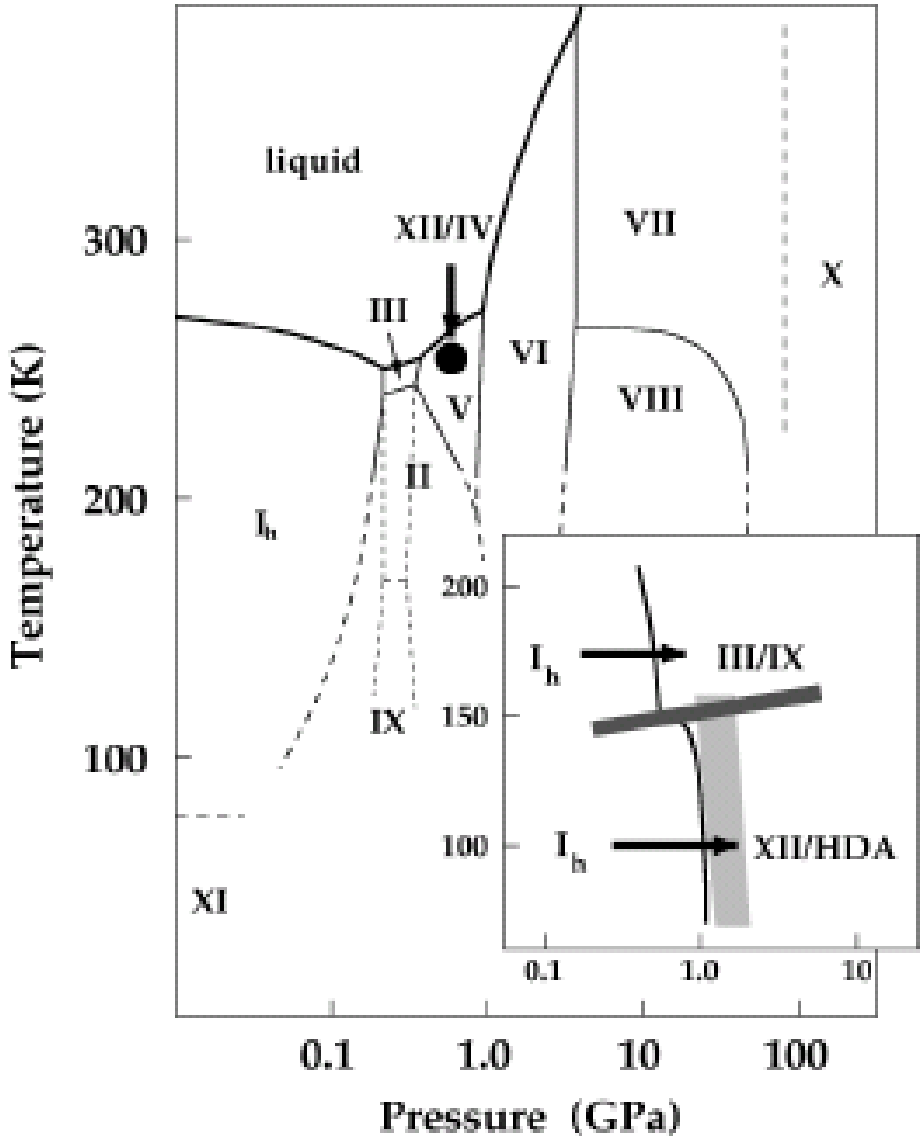


**The phase diagram of ice.**

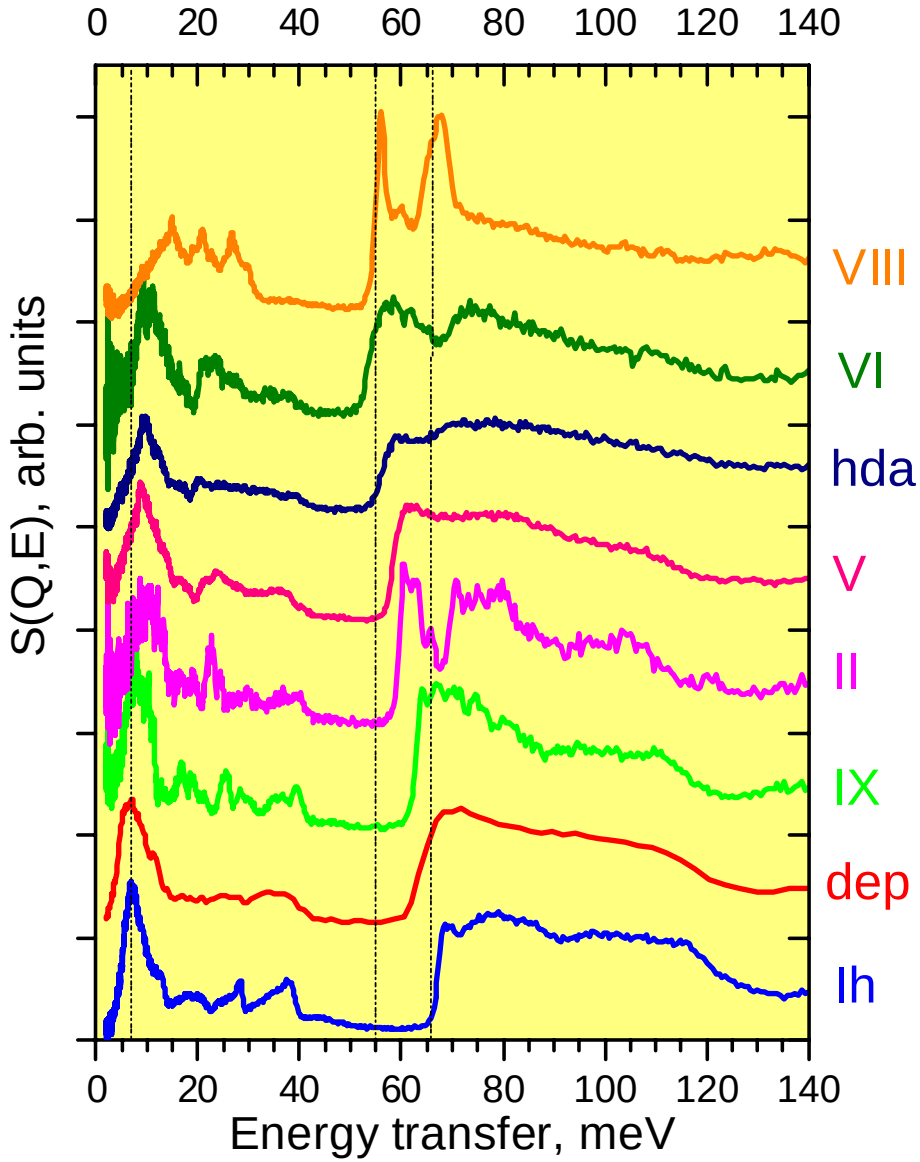


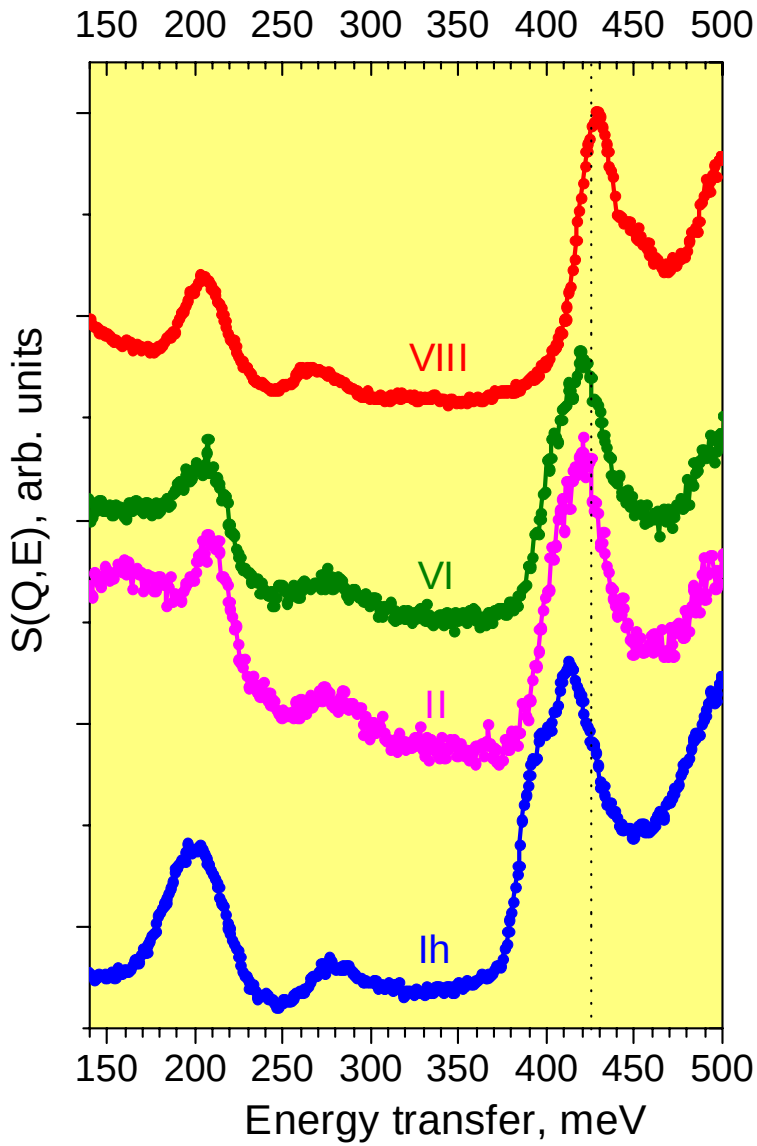


Inelastic neutron scattering spectra of different ice phases

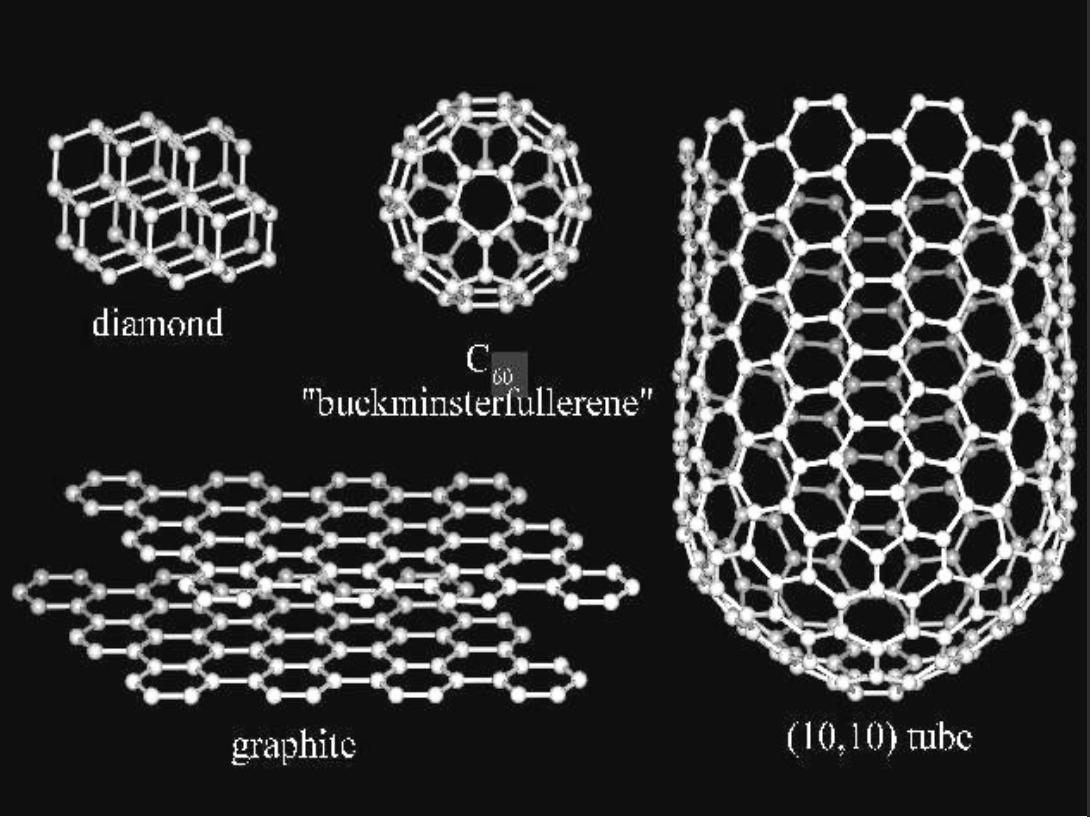


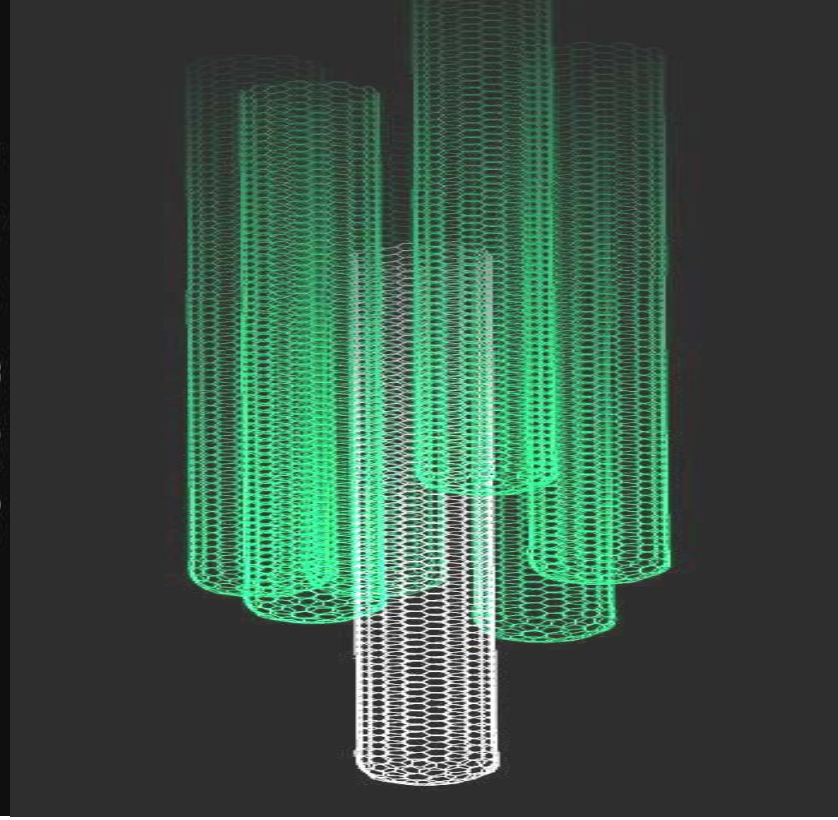

**Four perfect crystalline forms of carbon: diamond, graphite, C60, and a (10,10) single walled nanotube. (From the Nobel Lecture, December 7, 1996, by Richard E. Smalley).**

**In 1991 Iijima observed for the first time tubular carbon structures – multi-walled carbon nanotuebs (MWNT), cylindrical tubes consisting of rolled graphene sheets.**

**Two year later Iijima & Ichihashi, and Bethune *et al*. synthesized single-walled carbon nanotubes (SWNT).**

***Can water enter the SWNT of inner diameter 14 Å?***

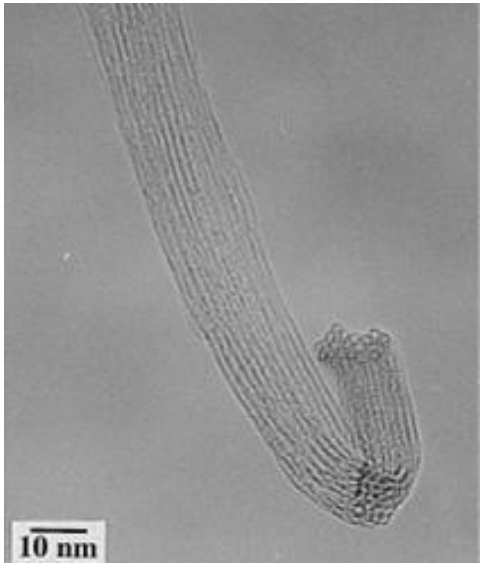


TEM picture of SWNT bundles.



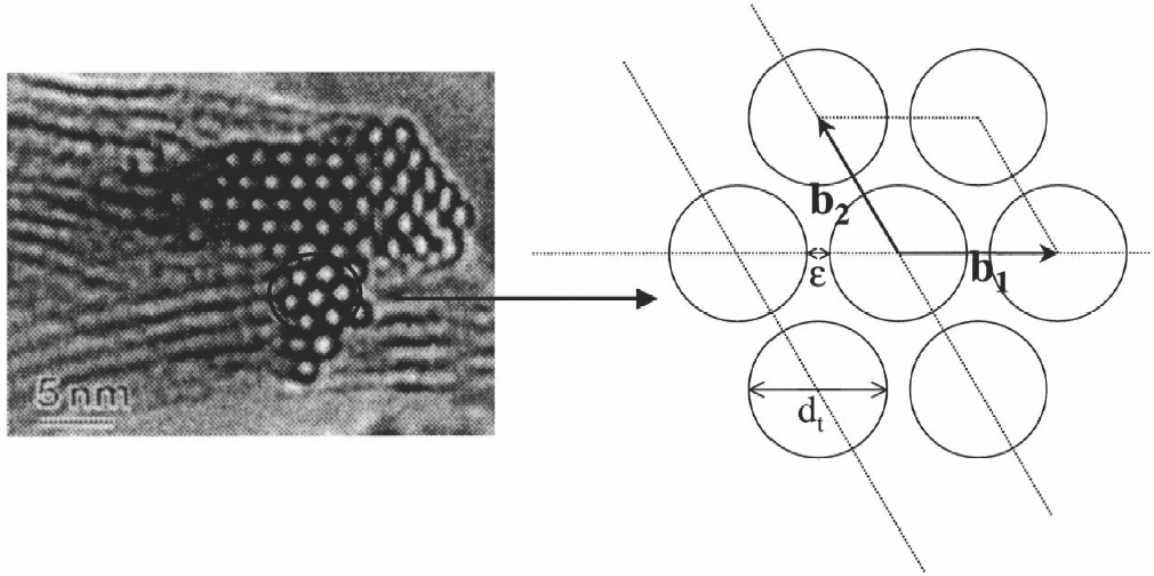


Fig. 1. Left: transmission electron microscopy observation of crystalline packing of SWNT in bundles (from Ref. [10]). Right: sketch of the 2D hexagonal lattice.

**SWNT sample (m=3.8 g) with D≈14±1 Å, l~10 µm** was produced by MER and characterized by HRTEM, TEM, SEM, Raman and ND measurements.

To fill the SWNT with water, the dry SWNT sample was first exposed to saturated vapor from a water bath (1:1 weight ratio) at 110°C for 2 hours in an enclosed environment. The excess water adsorbed in the exterior of the nanotubes was then evaporated at 45°C. An optimal filling, in terms of $H_2O$/SWNT mass ratio was found to be 11.3%.

# *Water Enters the Nanotubes by Exposing SWNT to Water Vapor at ~110°C*

Low-angle neutron diffraction: $I(Q) \sim S(Q) \bullet F(Q)$. Here, $S(Q)$ consists of a Bragg reflection at 0.41 $Å^{-1}$ from the (01) planes of the 2D hexagonal lattice of SWNT crystalline bundles.

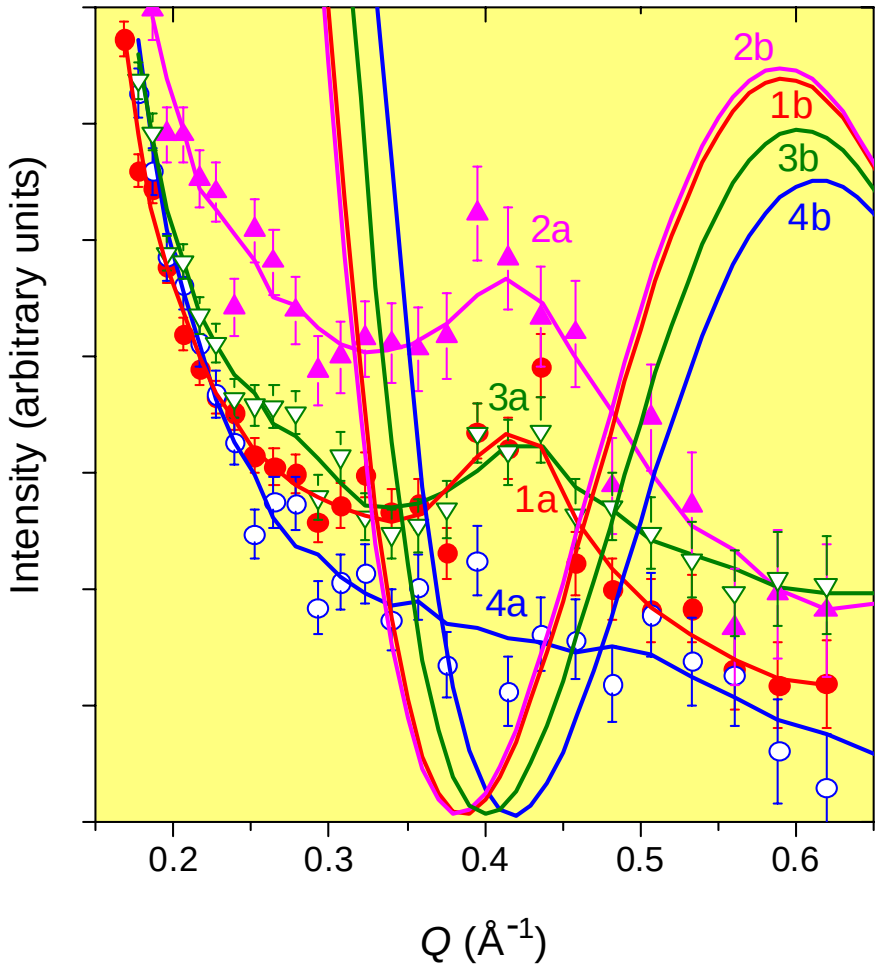


**1 – Dry SWNT**

**2 – SWNT & $H_2O$**

**3 – SWNT & $(H_2O)_{0.5}(D_2O)_{0.5}$**

**4 – SWNT & $D_2O$**

**SAND, IPNS**

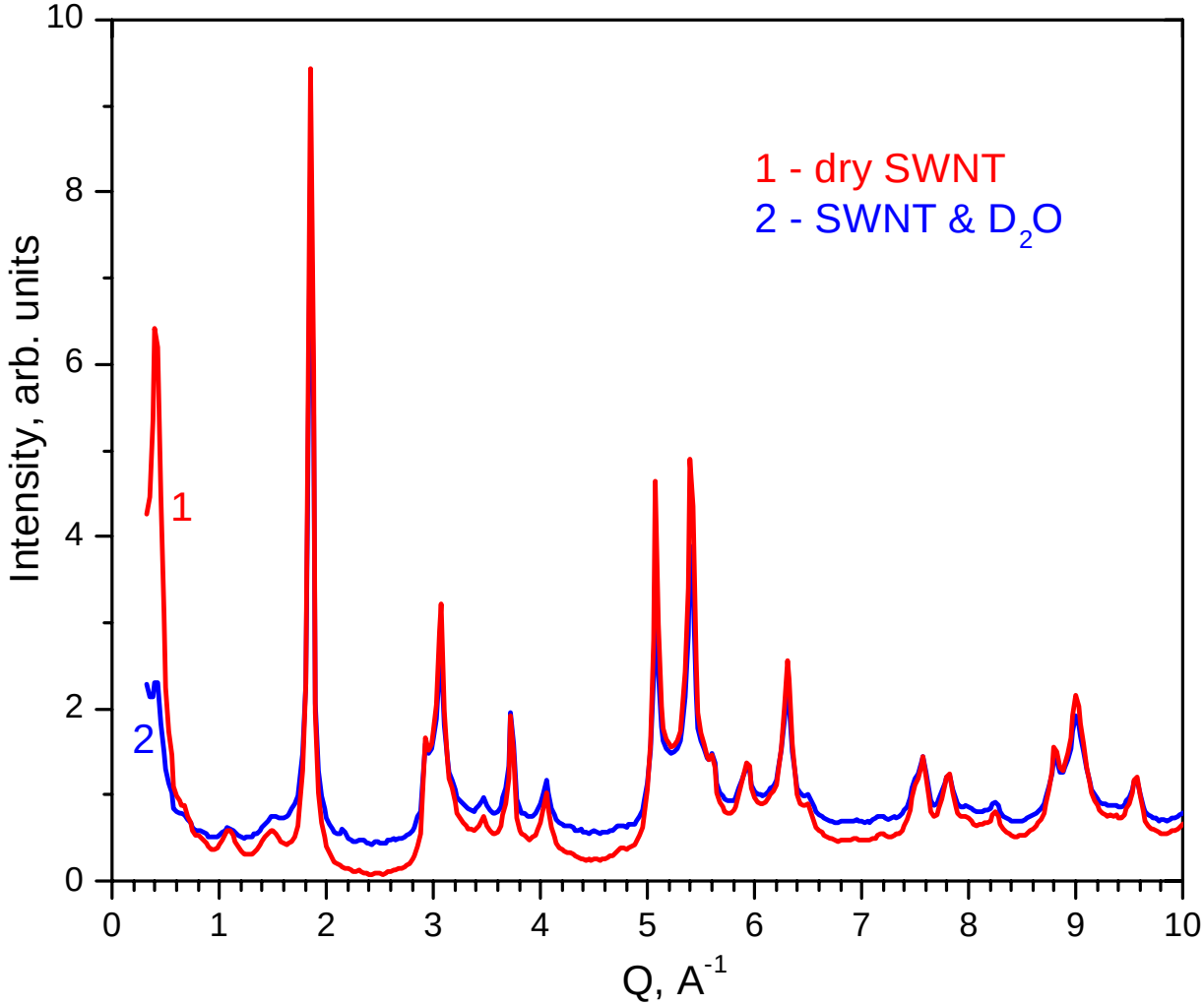


ND profiles of dry SWNT and SWNT & $D_2O$ at 10 K measured on GLAD (IPNS).

***What are the effects of nanotube confinement on the dynamics of water?***

# *Strong Renormalization of the Low-Energy Intermolecular Vibrational Density of States*

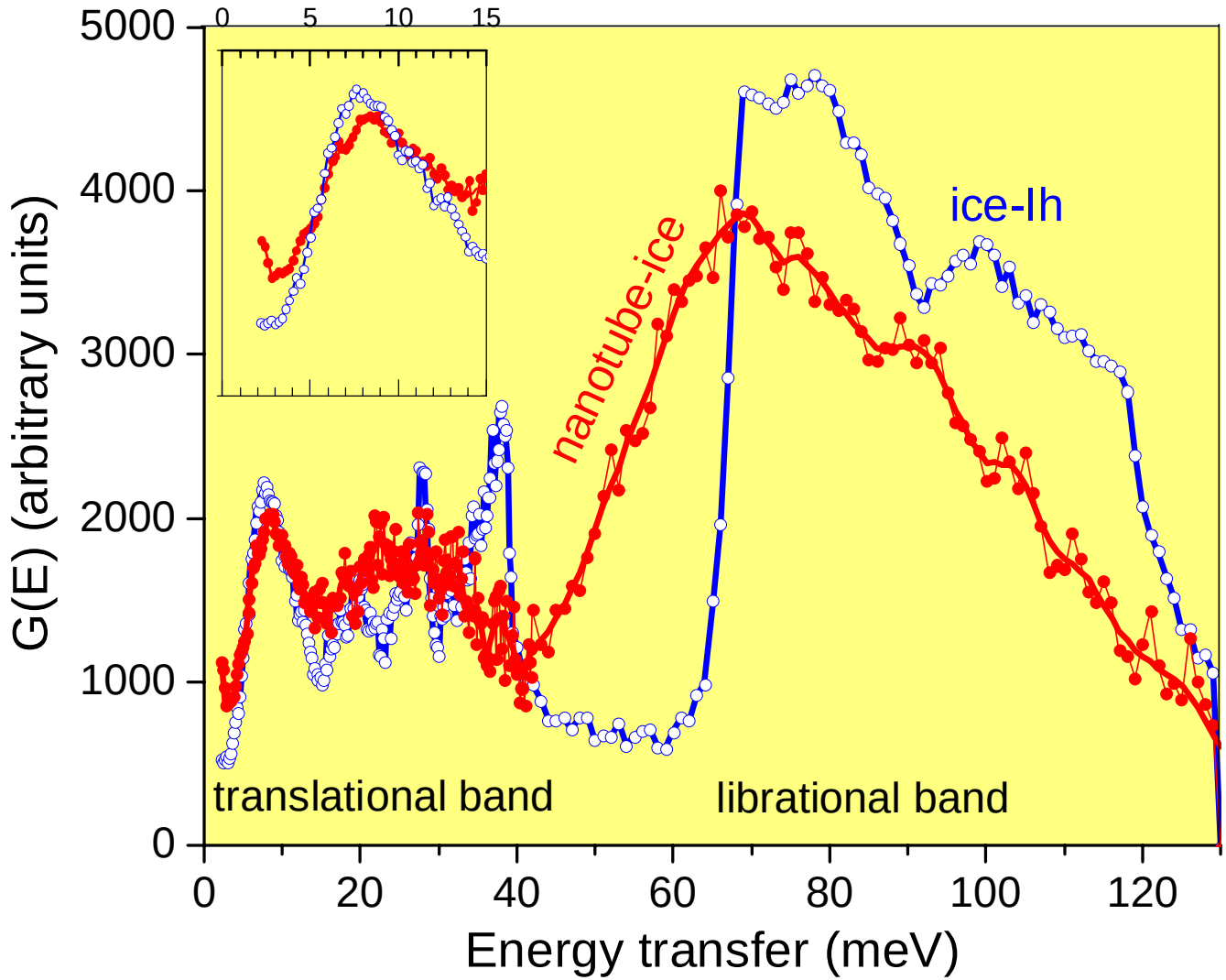

# *A Significantly Weaken Hydrogen-Bond Network in Nanotube-Water*

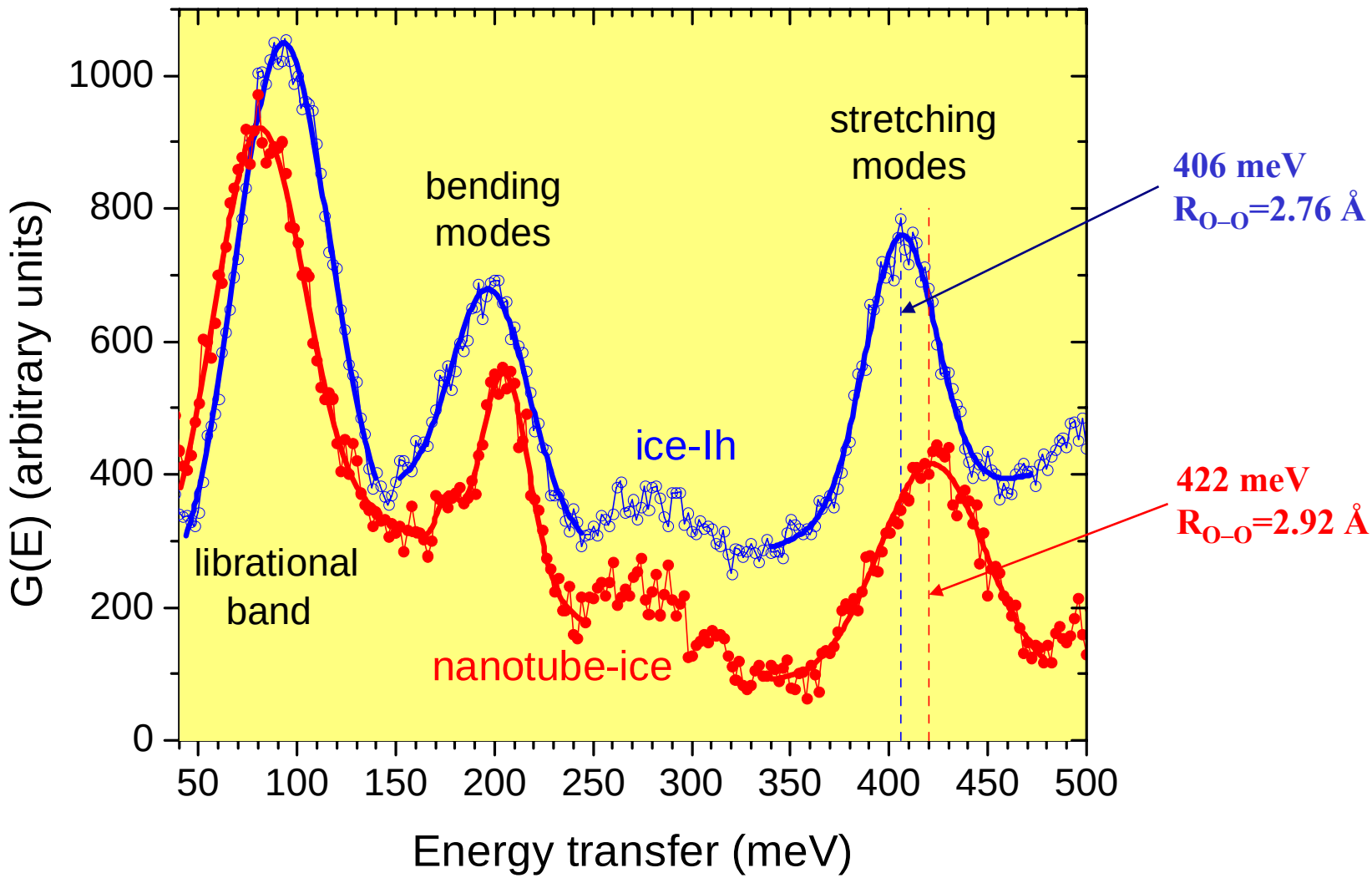

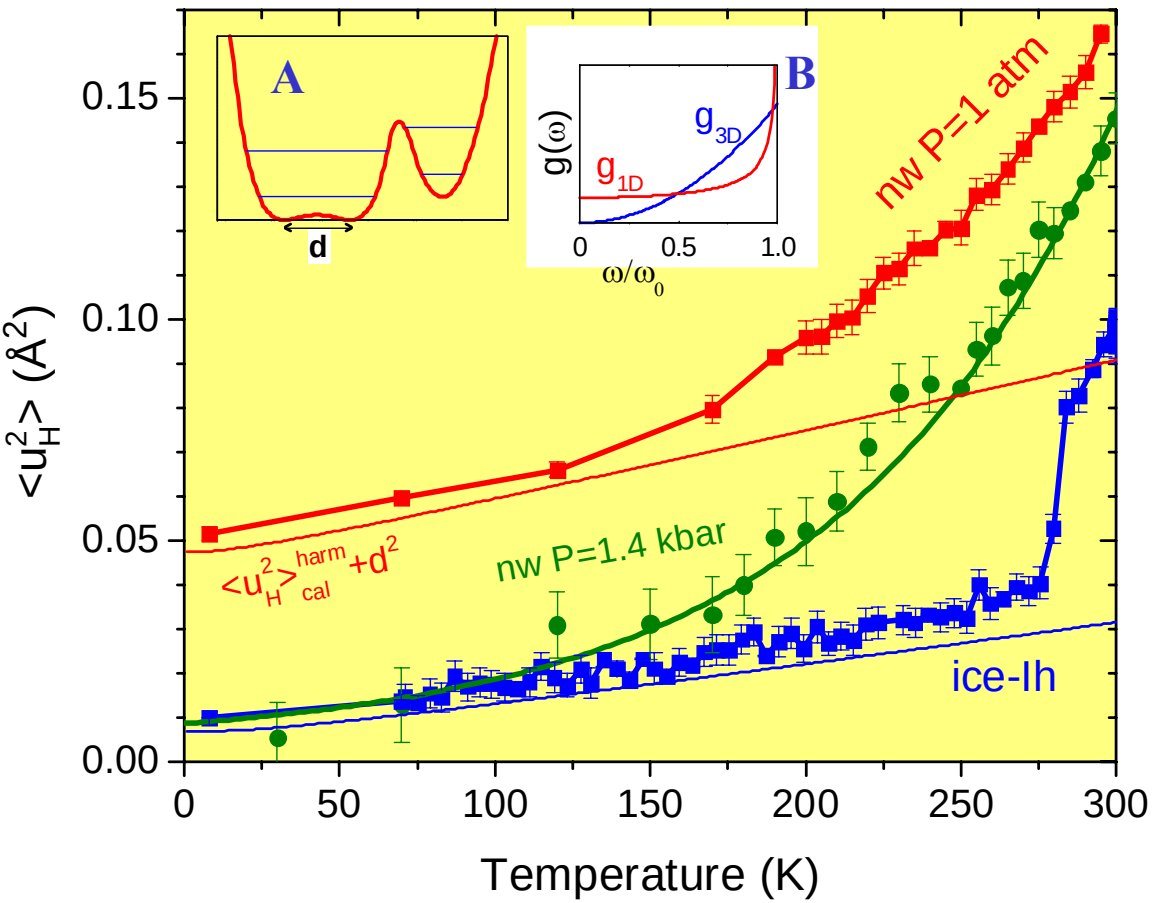


Red and blue solid lines show the $\langle u_H^2 \rangle$ calculated in an harmonic approximation using the measured $G(E)$. To describe the $\langle u_H^2 \rangle$ for nanotubes-water the calculated curve was vertically shifted by supposed delocalization, $d$~0.2 Å, of the hydrogen atoms due to the flatten bottom of its potential (insert A). Insert B shows another possible scenario, when the large $\langle u_H^2 \rangle$ in quasi 1D nanotube-water can be originated from finite value of the $g(\omega)$ at low energies in 1D chain, $g(\omega) \sim (\omega_0^2 - \omega^2)^{-1/2}$, compared to $g(\omega) \sim \omega^2$ behavior for the bulk 3D case.

$\langle u_H^2 \rangle$ for nanotube-water under pressure P=1.4 kbar below 100 K is reduced drastically to values comparable to those in ice-Ih. At higher temperatures it rises very rapidly above the ice-Ih value. Data show no abrupt transition near 273 K.

# *Summary: Experimental Observation*

- **Water enters the single-walled carbon nanotubes at about ambient condition, likewise in many biological counterparts such as aquaporin, gramiciden and bacteriorhodosin.**

- **The hydrogen-bond energetics of water confined within nanotubes is significantly modified. The blue shift of intramolecular vibrations and red-shift of intermolecular bands indicate more pliable hydrogen bonds.**

- **Nanotube-water is extraordinary "soft" - hydrogen atoms may be considered as situated in a strongly anharmonic potential well, implying a higher diffusion rate of protons. An applied pressure (1.4 kbar) first suppresses the soft dynamics below ~150 K but gives way to thermal excitations at higher temperatures.**

# *MD simulations and proposed nanotube-water structure.*

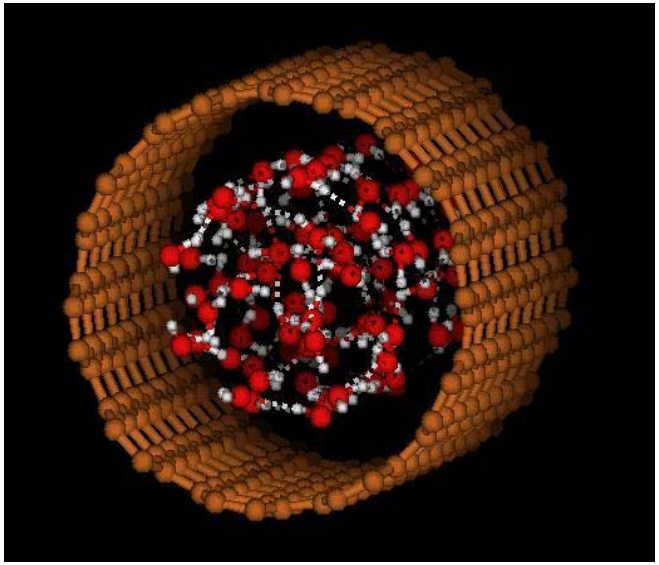

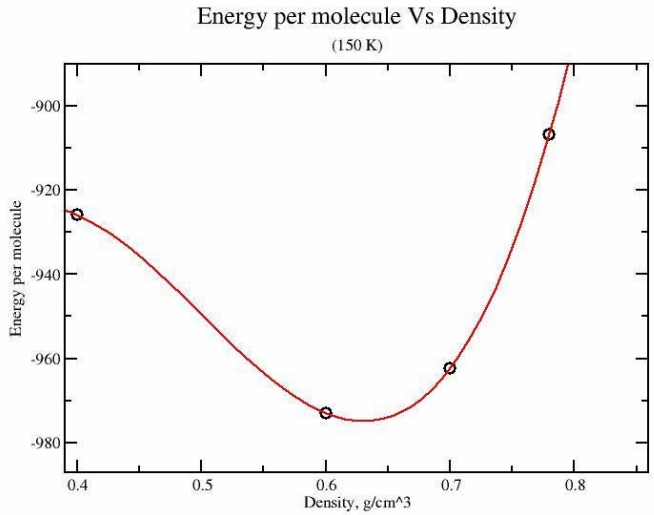


MD calculations for water in SWNT have been performed using the **TTM2-F polarizable flexible water model** of Burnham and Xantheas (uses smeared charges and dipoles to model short range electrostatics) [1]. This model has been shown to be in excellent agreement with high-level electronic structure data for small water clusters and can also reproduce bulk behavior of ice and ambient liquid water.

Our MD simulations consist of a rigid carbon nanotube of length 40 Å in periodic boundary conditions that interacts with waters through the Lennard-Jones potential (from Ref. 2). An Ewald sum was used for the long-range Coulomb interactions.

We initially attempted slow simulated annealings at a range of different water densities in order to find candidate structures with the lowest energy per water-molecule.

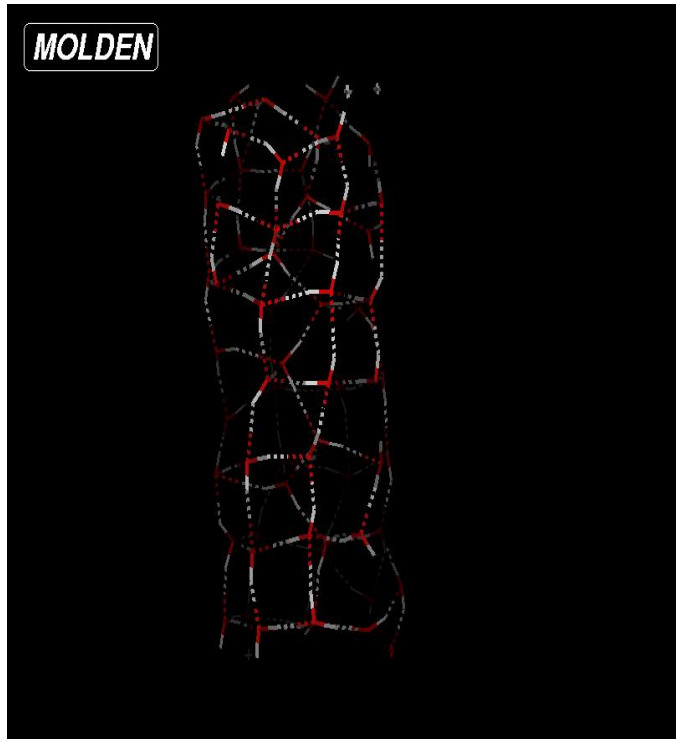


1. C.J. Burnham and S.S. Xantheas, J. Chem. Phys. **116** (2002) 1500, 5115
2. J.H. Walther et al., J. Phys. Chem. B **105** (2001) 9980

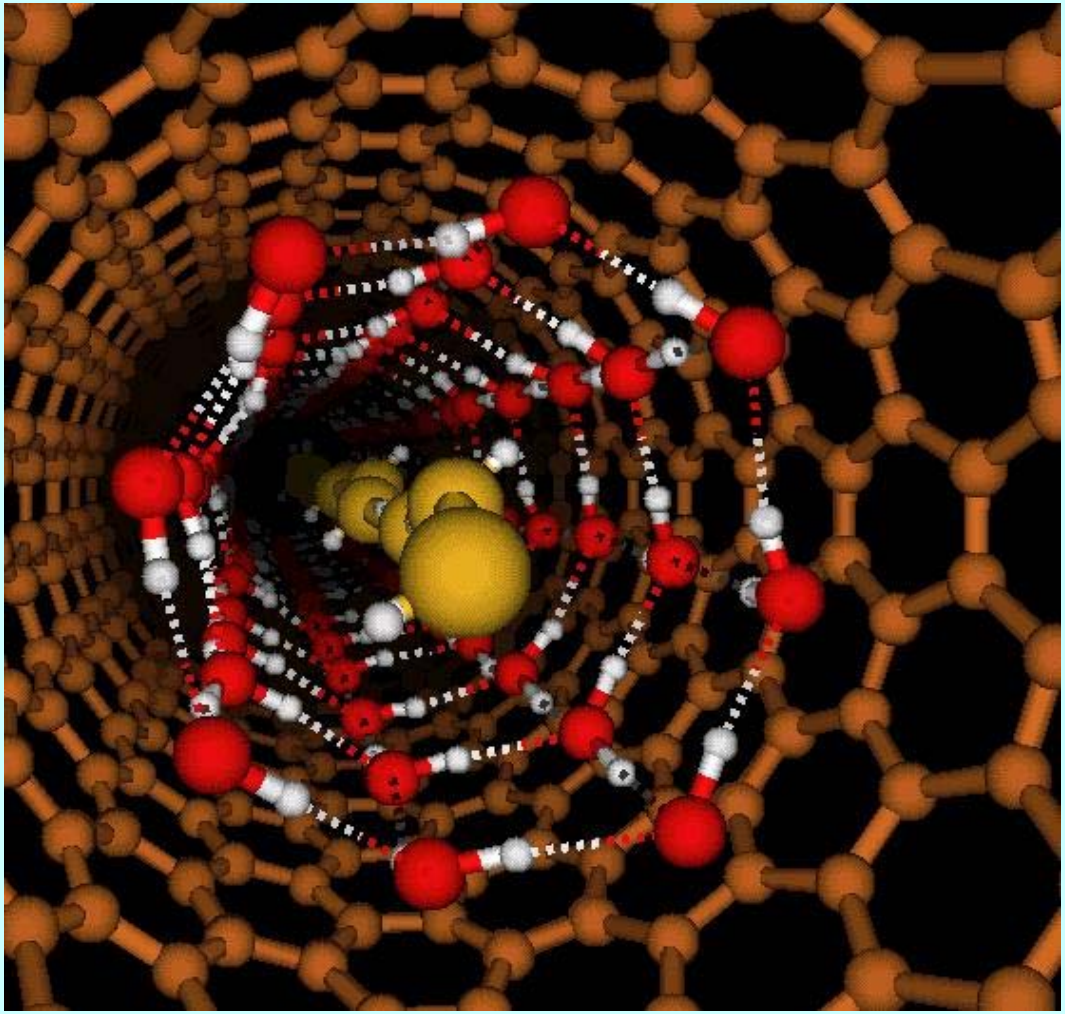

**Proposed structure of nanotube-water. The interior "chain" water molecules have been colored yellow to distinguish them from the exterior "wall" water molecules (colored red).**

Succinyl linked gramicidin A channel in GMO bilayer (From simulation by Zhen Qin)

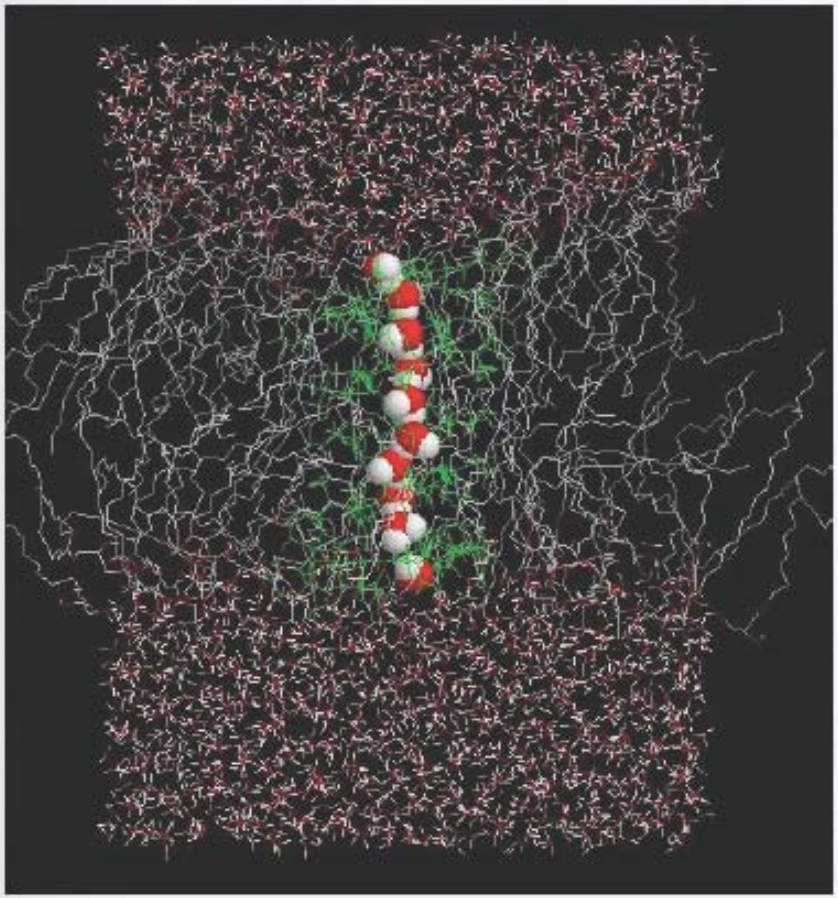

Proposed Nano-ice structure

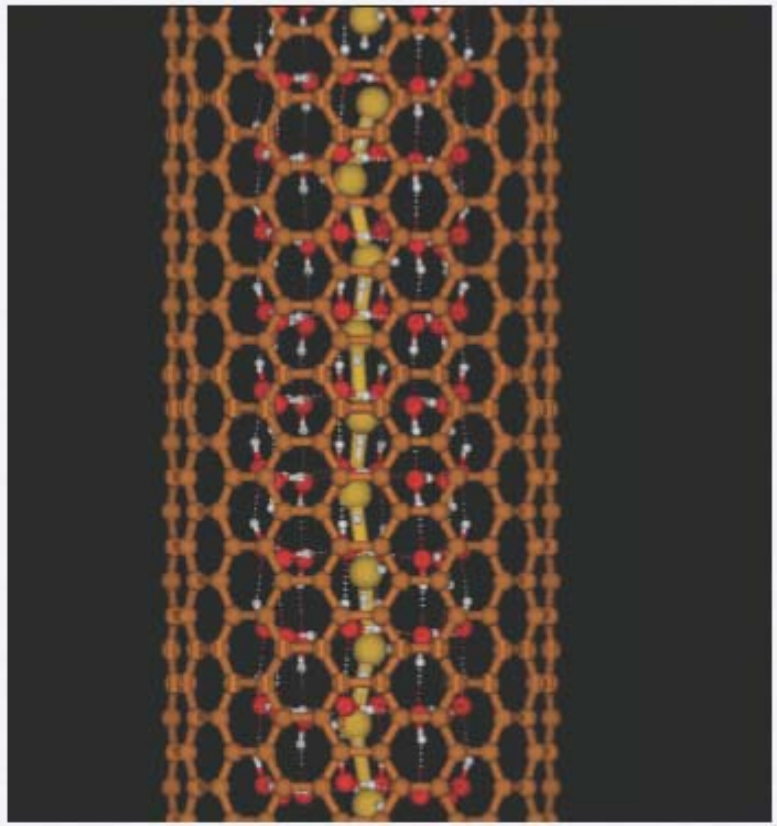

Reminiscent of biological water channels.

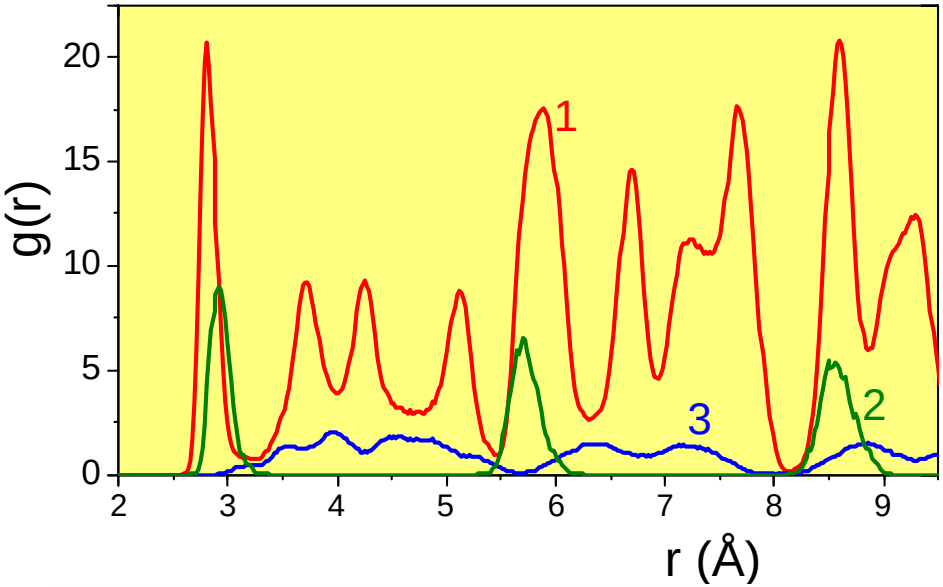


**1 – wall water**
**2 – chain water**
**3 – chain-wall**

Calculated O-O RDF functions for nanotube-water.

Chain and wall waters are very structured.

Very little structure between **chain and wall** water molecules.

Chain molecules have less than 2-fold coordination – much less than in the bulk liquid.

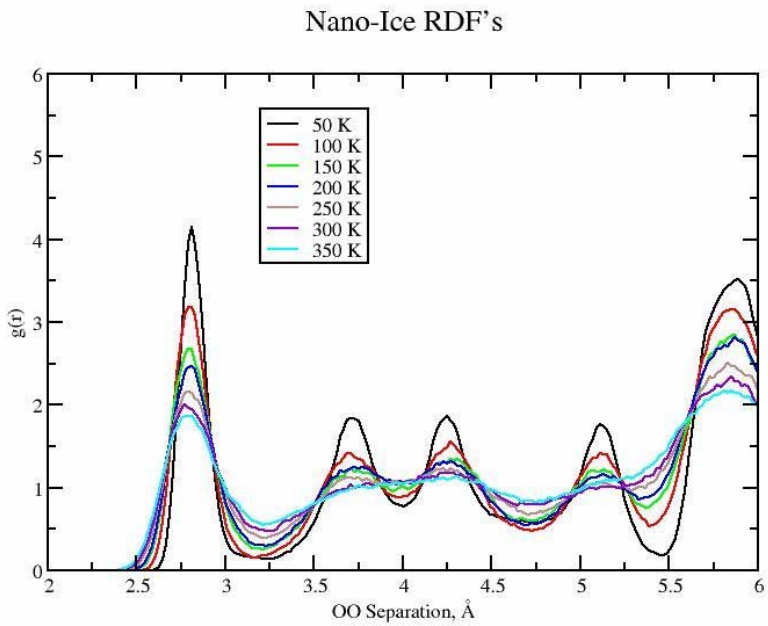


Temperature behavior of calculated RDF function for nanotube-water

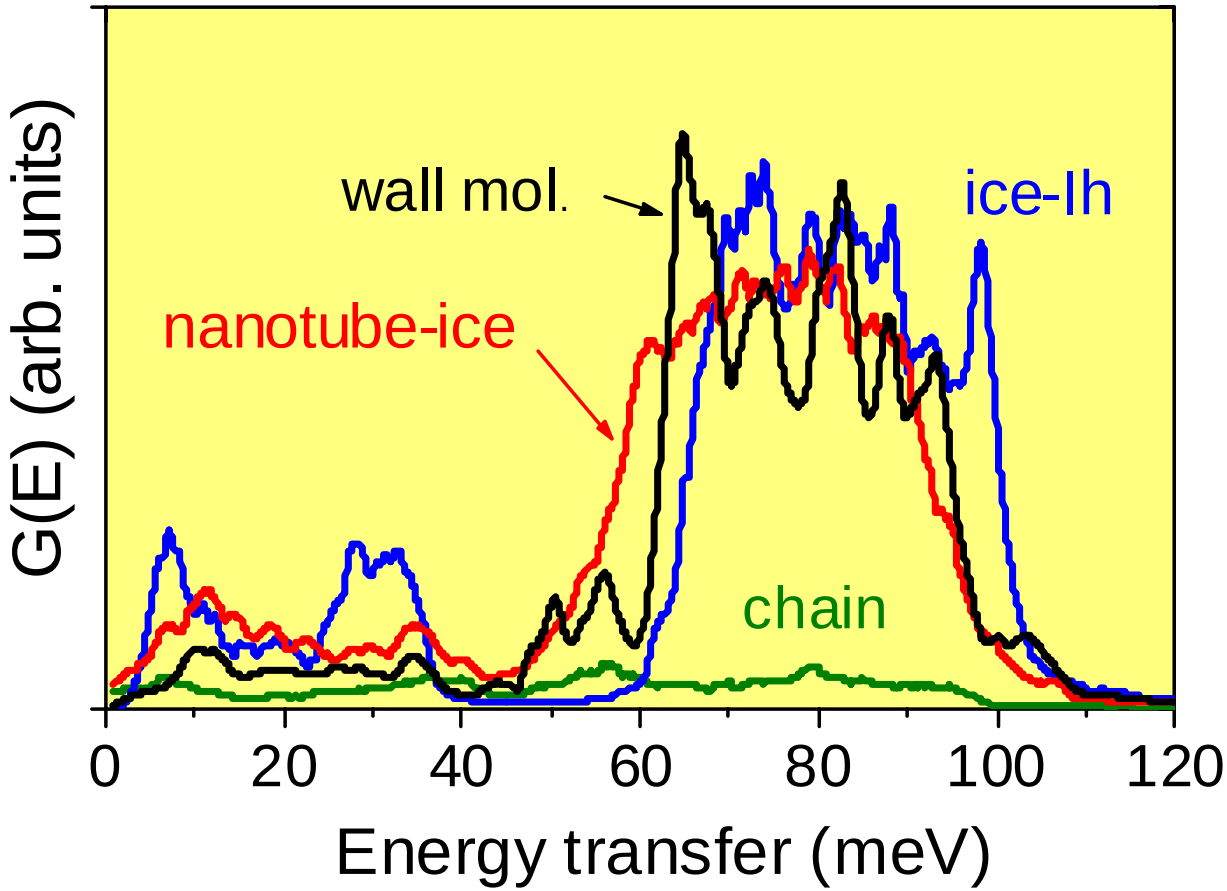


Calculated vibrational spectra for nanotube-ice, wall molecules alone and chain water in nanotube-ice, compared with ice-Ih.

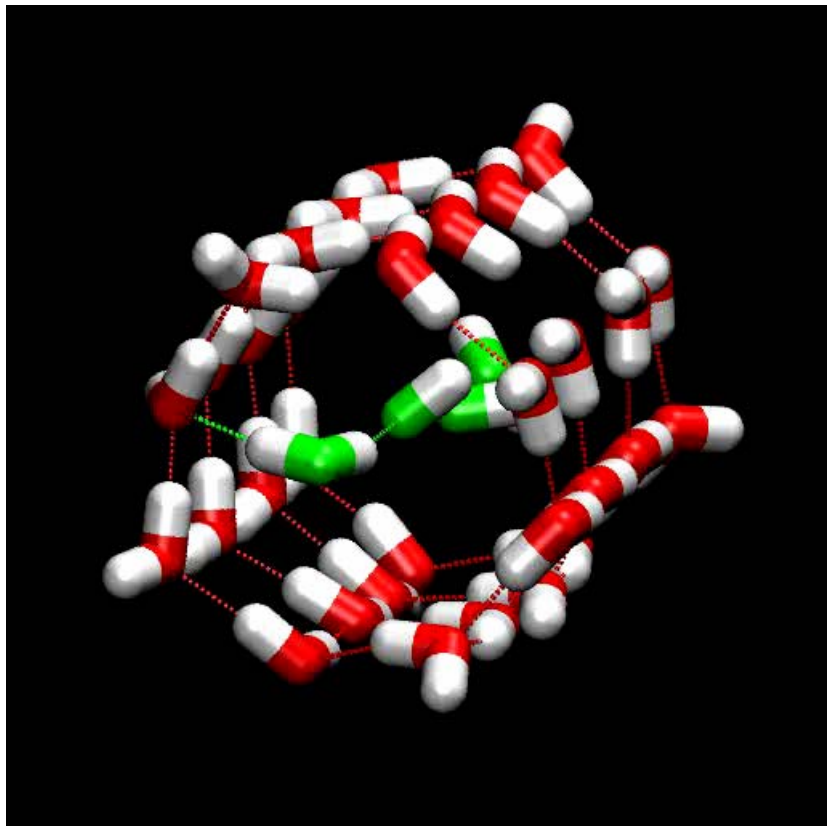

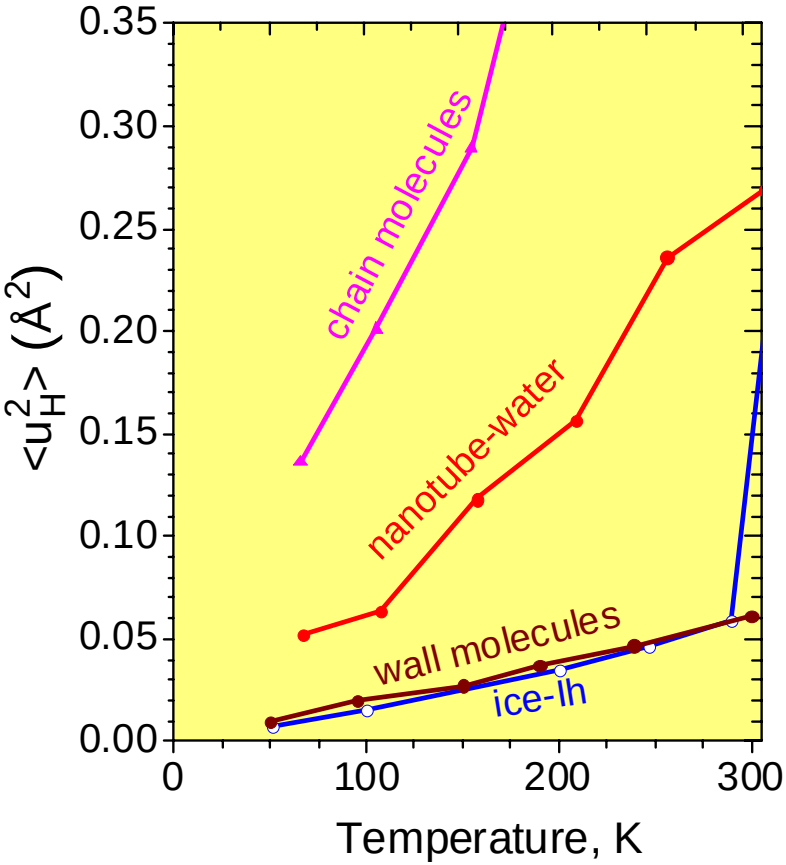


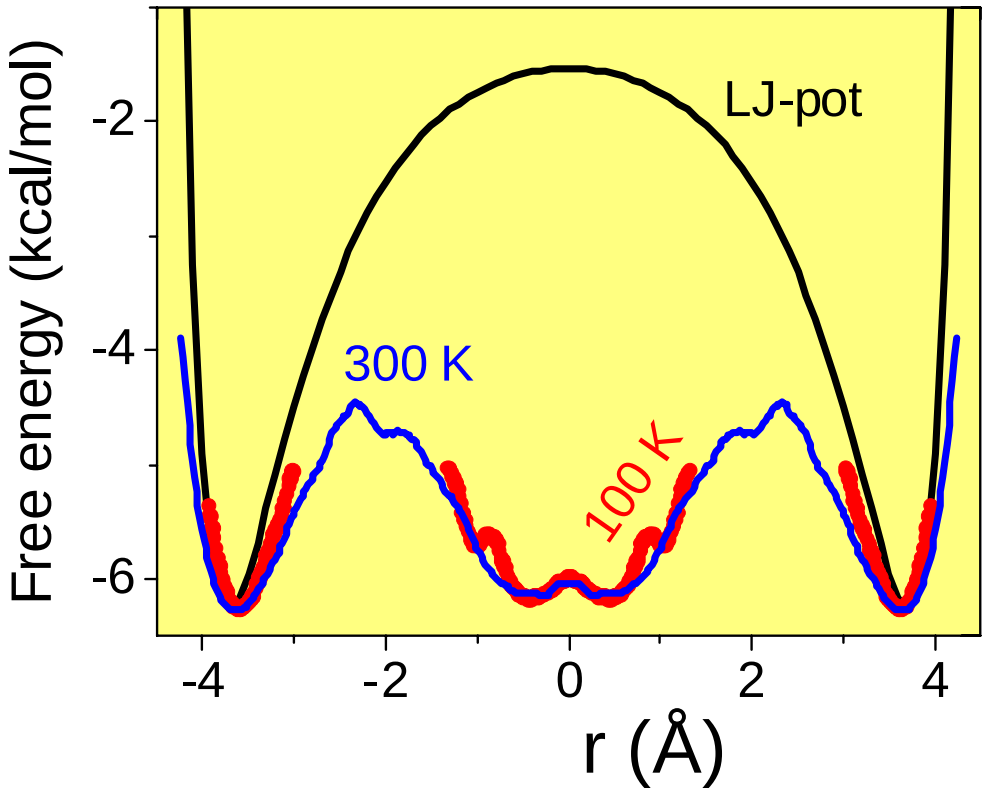


Calculated $\langle u_H^2 \rangle$ for nanotube-ice, wall molecules alone and chain water in nanotube-ice, compared with ice-Ih.

Free energies across the nanotube walls for water molecules in nanotube-water/ice at 100 K (red) and 300 K (blue). The L-J potential (black) provides the minima for location of individual water molecules initially entering the SWNT.

# Summary

☺ ***ND measurements clearly demonstrated the entry of water into SWNT.***

☺ ***INS measurements showed very soft dynamics of nanotube-water.***

☺ ***MD simulations identified an ice-wall plus water-chain structure. The soft dynamics of nanotube-water arises mainly from the drastic change in hydrogen-bond connectivity of the central water-chain with an average coordination number of 1.86.***

☺ ***Anomalously enhanced thermal motions in the water-chain, interpreted by a low-barrier, flattened, highly anharmonic potential well, explains the large $\langle u_H^2 \rangle$ and fluid-like behavior of nanotube-water at low temperatures.***

*This behavior agrees qualitatively with the expected water transport via the nominally hydrophobic inner region of transmembrane proteins such as aquaporin, gramicidin, and bacteriorhodosin [Y. Kong and J. Ma, Proc. Natl. Acad. Sci. USA 98, 14345 (2001); R. Pomes and B. Roux, Biophys. J. 82, 2304 (2002); J.K. Lanyi, J. Phys. Chem. B 104, 11441 (2000)].*

# *Further Studies*

- **Water in carbon nanotubes of different diameter (8 Å, 16 Å).**
- **Pressure effect (up to 5 kbar). A possible existence of a new critical point?**
- **QENS study of water in SWNT using back-scattering spectrometer and DCS at NIST.**
- **Neutron Compton scattering on water in SWNT.**
- **MD simulations for water at different pressures, temperatures and for different nanotube radii, attempt to model zero-point effects.**

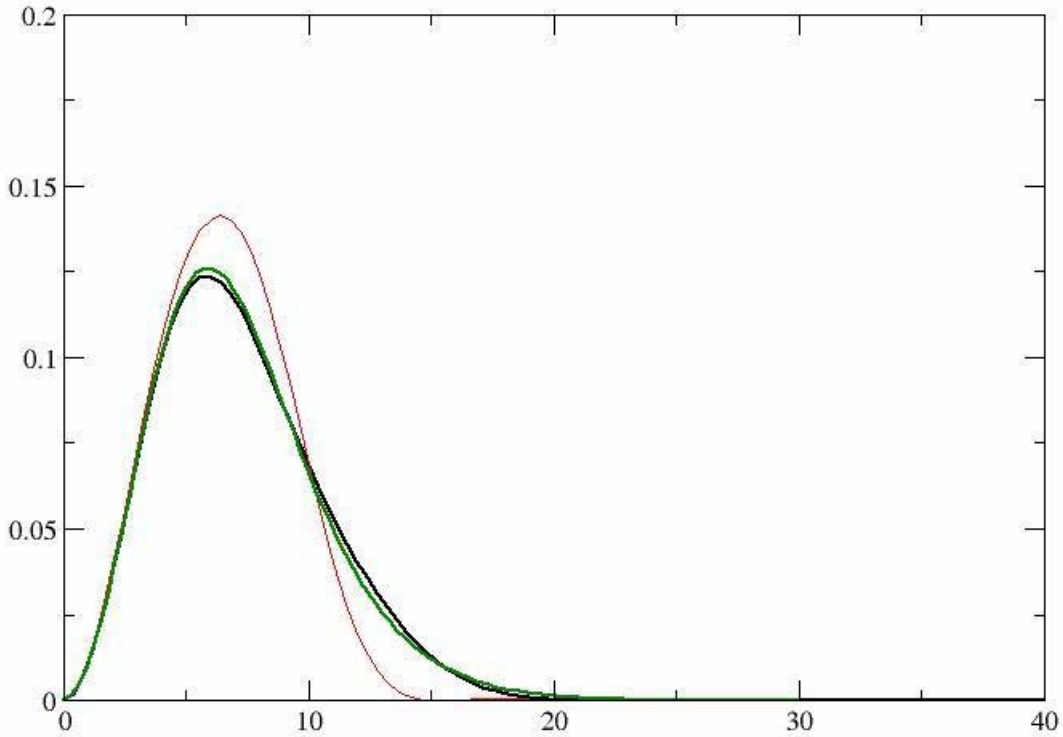


Proton Momentum Distribution in nanotube-water at 4 K (red curve) and ice at 269 K measured on VESUVIO spectrometer at ISIS. Nanotube-water spectrum is clearly much narrower, hence more spread out in space.

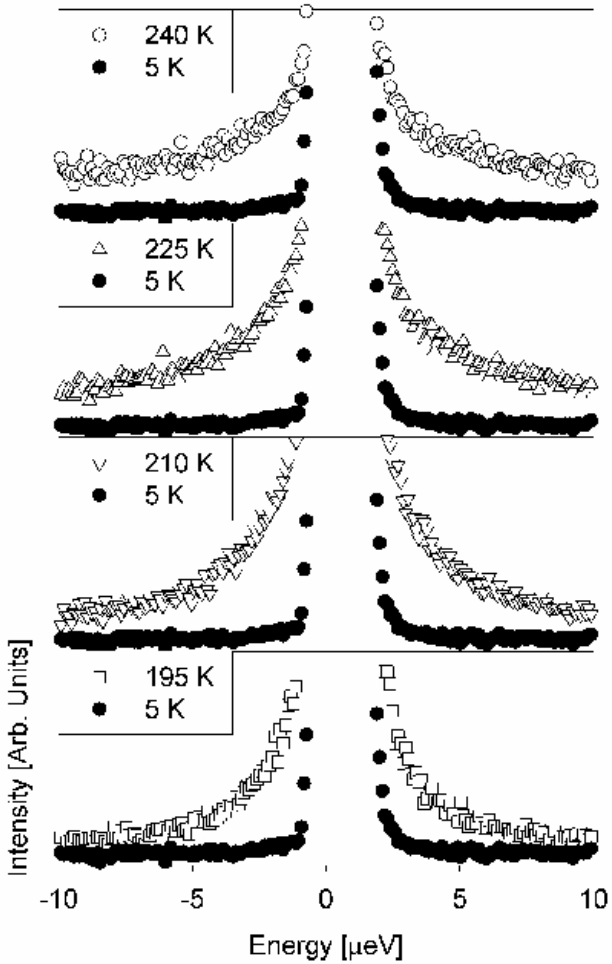


**Q=0.99 Å$^{-1}$**

**QENS on water in DWNT measured at back-scattering spectrometer at NIST**

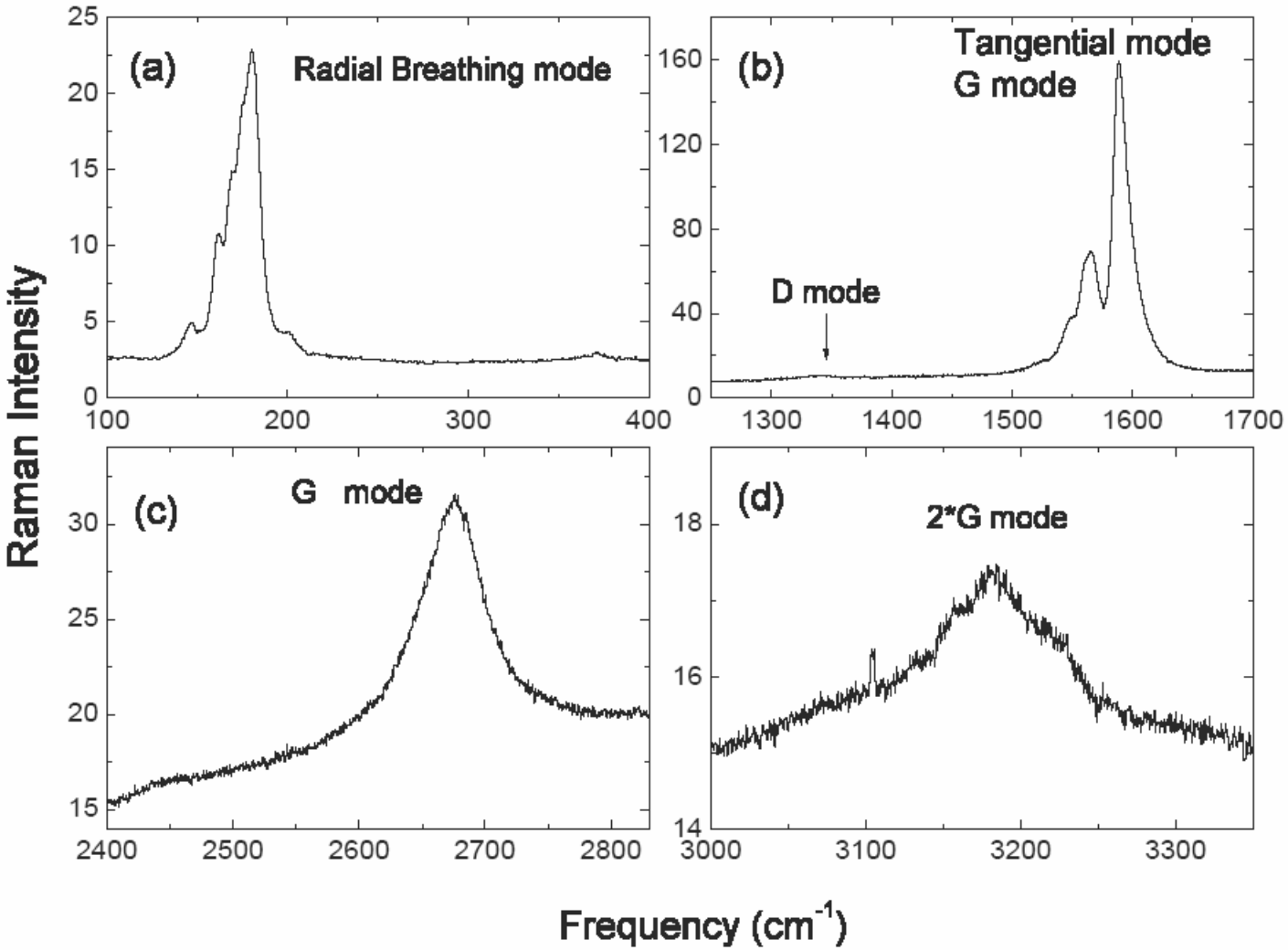


A.G.Souza Filho, Departamento de Fisica, Universidade Federal do Ceará, Fortaleza – Ceará, Brazil

The form-factor can be calculated as following (S. Kline and A. Munter, 1999):

$$P(q) = \frac{scale}{V_{shell}} \int_0^{\pi/2} f^2(q,\alpha) \sin\alpha \, d\alpha$$

$$f(q,\alpha) = 2(\rho_{core} - \rho_{shell}) V_{core} j_0(qH\cos\alpha) \frac{J_1(qr\sin\alpha)}{(qr\sin\alpha)}$$

$$+2(\rho_{shell} - \rho_{solvent}) V_{shell} j_0[q(H+t)\cos\alpha] \frac{J_1[q(r+t)\sin\alpha]}{[q(r+t)\sin\alpha]}$$

$$j_0(x) = \sin(x)/x \qquad V_{core} = \pi r^2 L \qquad V_{shell} = \pi(r+t)^2 L_{total}$$

, where $r$ is the radius of the core of the cylinder, and $J_1(x)$ is the first order Bessel function. Alpha is defined as the angle between the cylinder axis and the scattering vector, **q**.

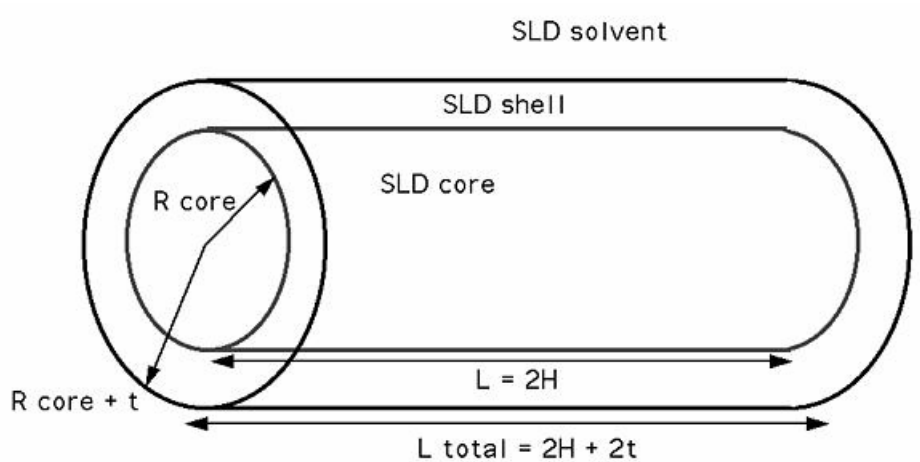

# GLAD, IPNS

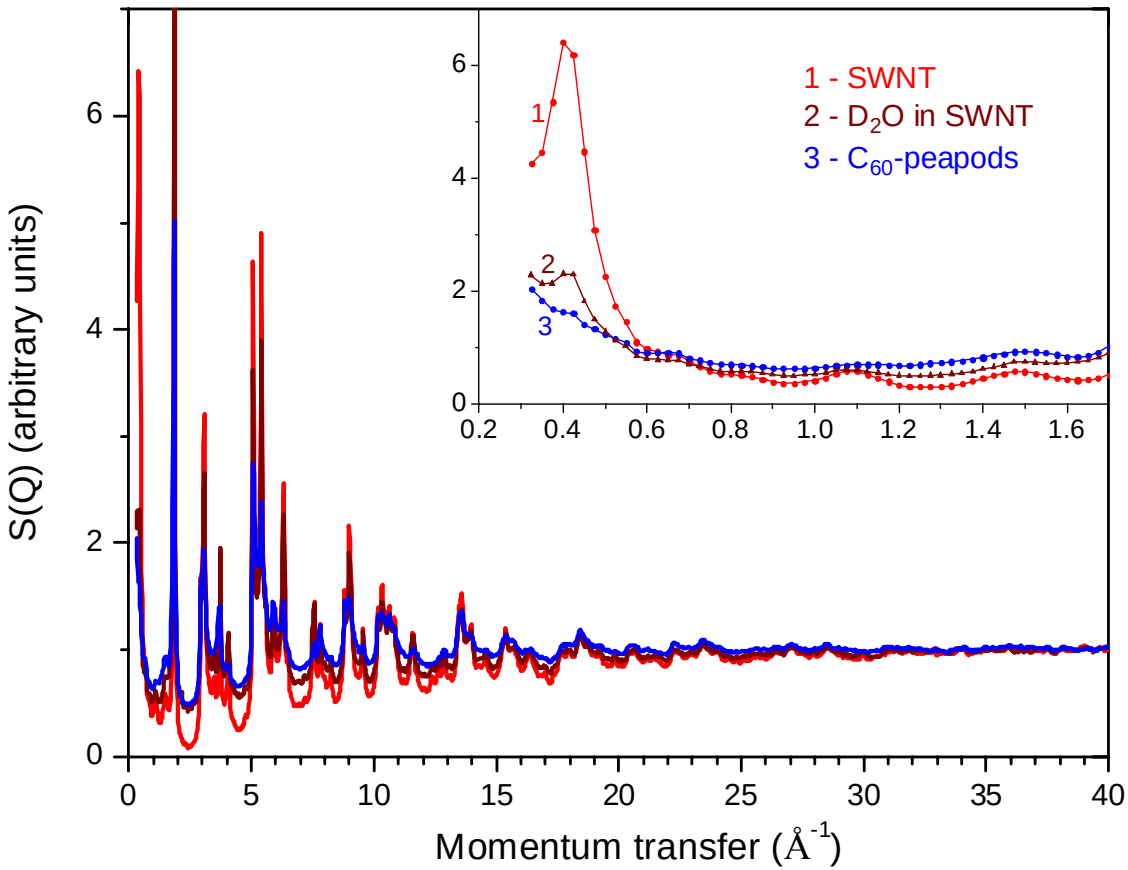


# SAND, IPNS

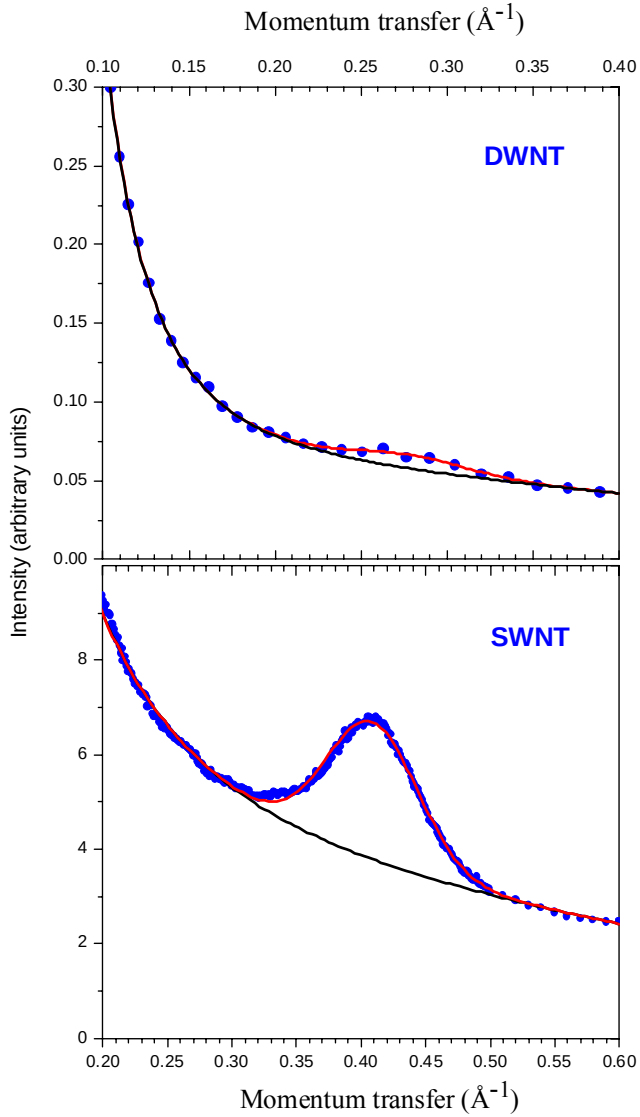

The quantity measured in the inelastic neutron scattering experiment is the double differential cross section

$$\frac{d^2\sigma}{d\Omega d\omega} = \frac{k_f}{k_i} S(\mathbf{Q},\omega) = \frac{k_f}{k_i} \sum_{ij} \int_{-\infty}^{\infty} < b_i b_j^* e^{i\mathbf{Q}\mathbf{r}_i(0)} e^{-i\mathbf{Q}\mathbf{r}_j(t)} > e^{i\omega t} dt$$

The scattering function $S(\mathbf{Q},\omega)$ provides the link between the scattering data and the physical system being studied. The type of experiment dictates the portions of $(\mathbf{Q},\omega)$ space which have to be probed.

$$\mathbf{r}_i(t) = \mathbf{R}_i + \mathbf{u}_i(t)$$

$$S(Q,\omega) = S(Q,\omega)^{inc} + S(Q,\omega)^{coh} =$$

$$\sum_i \sigma_i^{inc} \frac{\hbar}{6NM_i} \exp(-2W_i) \sum_{l,q} \frac{|\mathbf{Q}\cdot\mathbf{e}_i(l,q)|^2}{\omega(l,q)} (n_B + 1) +$$

$$\frac{\hbar}{6N} \sum_{i,j} \overline{b}_i \overline{b}_j e^{-(W_i+W_j)} e^{i\mathbf{Q}(\mathbf{R}_i-\mathbf{R}_j)} \sum_{l,q} \frac{[\mathbf{Q}\cdot\mathbf{e}_i(l,q)][\mathbf{Q}\cdot\mathbf{e}_j(l,q)]}{\sqrt{M_i M_j}\,\omega(l,q)} (n_B + 1),$$

$$S_{1ph}^{inc}(Q,\omega) = \sum_i \sigma_i \frac{\hbar Q^2}{2M_i} \exp(-2W_i) \frac{G_i(\omega)}{\omega} [n_B(\omega)+1]$$

$$G(\omega) = \sum_i G_i(\omega) = \sum_{i,l,\boldsymbol{q}} \frac{1}{3N} \left|\boldsymbol{e}_i(l,\boldsymbol{q})\right|^2 \delta[\omega - \omega(j,\boldsymbol{q})]$$

$$W_i = \frac{1}{2} < (\mathbf{Qu})^2 > = \frac{\hbar Q^2}{2M_i} \int \frac{G_i(\omega)}{\omega} [2n_B(\omega)+1] d\omega$$

The dynamical structure factor for hydrogen-containing materials can be written as the sum of INS contributions $S_{l,k-l}(Q, E)$, due to annihilation of $l$ and creation of $k-l$ excitations,

$$S(Q, E) = \sum_{l,k} S_{l,k-l}(Q, E) = \sum_{l,k} \frac{\sigma_{\mathrm{H}}^{inc}}{4\pi} \exp(-2W(Q)) \times \left(\frac{\hbar^2 Q^2}{6m}\right)^k \int \mathrm{d}\omega_1 \cdots \mathrm{d}\omega_k \frac{G(\omega_1) \cdots G(\omega_k)}{\omega_1 \cdots \omega_k (k-l)!\, l!} \times \prod_{i=l+1}^{k} [n_B(\omega_i) + 1] \prod_{j=1}^{l} n_B(\omega_j) \delta\left(E - \sum_{i=l+1,k} \hbar\omega_i + \sum_{j=1,l} \hbar\omega_j\right).$$

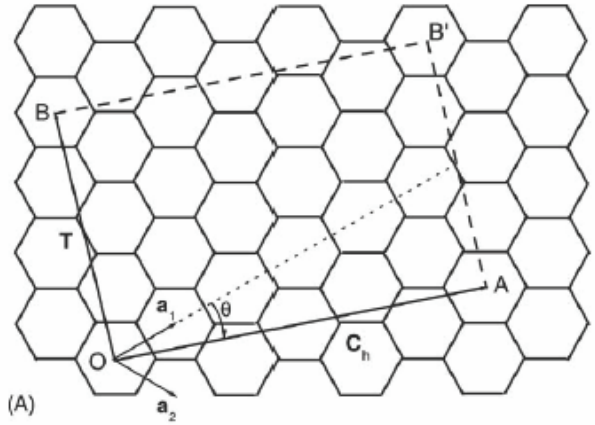


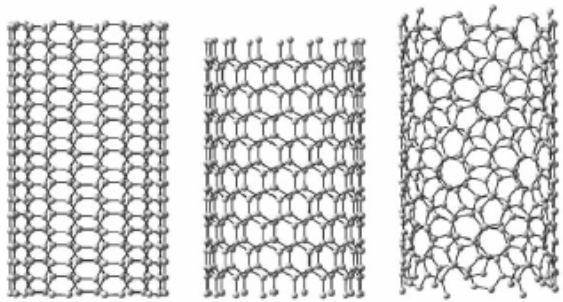


Fig. 1. Schematic representation of the construction of a nanotube by rolling-up an infinite strip of graphite sheet (so-called graphene). In (A) the chiral vector $\boldsymbol{C}_h = n\boldsymbol{a}_1 + m\boldsymbol{a}_2$ connects two lattice points O and A on the graphene sheet. An infinite strip is cut from the sheet through these two points, perpendicular to the chiral vector. The strip is then rolled-up into a seamless cylinder. $\boldsymbol{T} = t_1\boldsymbol{a}_1 + t_2\boldsymbol{a}_2$ is the primitive translation vector of the tube [5]. The nanotube is uniquely specified by the pair of integer numbers $n$, $m$ or by its radius $R = \boldsymbol{C}_h/2\pi$ and chiral angle $\theta$ which is the angle between $\boldsymbol{C}_h$ and the nearest zigzag of C–C bonds. All different tubes have angles $\theta$ between zero and 30°. Special tube types are the achiral tubes (tubes with mirror symmetry): armchair tubes $(n, n)$ $(\theta = 30°)$ (B(a)) and zigzag tubes $(n, 0)$ $(\theta = 0°)$ (B(b)). All other tubes are called chiral (B(c)). Details about relations between structural parameters of SWNTs can be found in [6].

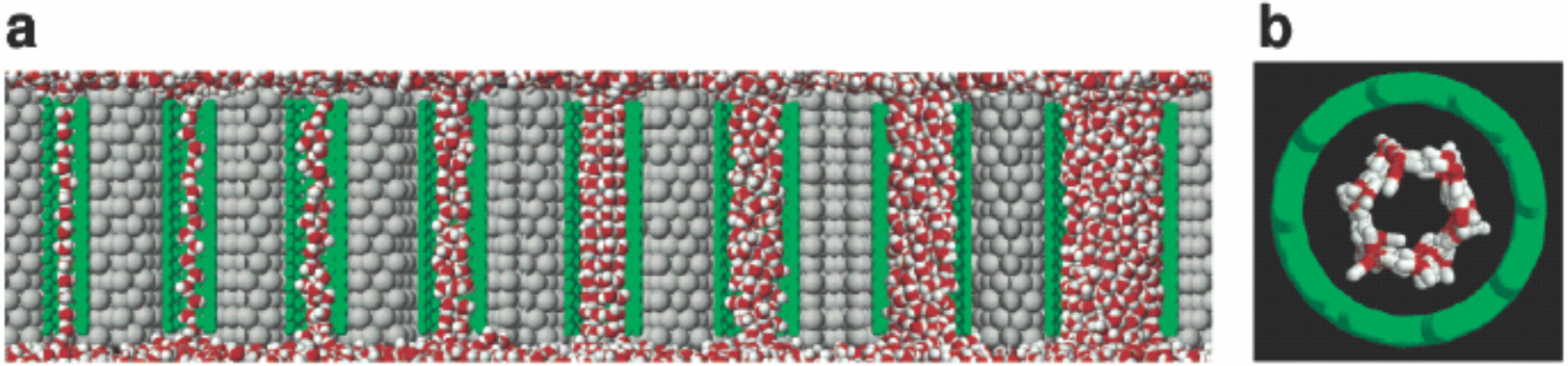


**Figure 1.** Snapshots from molecular dynamics simulations at 300 K. (a) Composite image of all systems (see Table) with nanotube size increasing from left to right. In narrow nanotubes, the water adopts a single-file arrangement but becomes more disordered in a fashion similar to that of bulk water in wider nanotubes. Confined within a nanotube of a "critical" diameter (fifth from left), the water spontaneously orders into a regular array. (b) Cross-sectional view of water inside the critical-sized 8.6-Å-diameter nanotube showing a multicolumnar water structure. Colors: nanotube (green), wafer (gray), water oxygens (red), water hydrogens (white). Images were derived from visualizations using RasMol.

"… the water generally shows **slowed dynamics compared to that of the bulk**, in nanotubes of a critical diameter it forms a structure resembling a stack of cyclic water hexamers exhibiting properties characteristic of both hexagonal ice and liquid water."

R.J. Mashl et al., Nano Lett. **3** (2003) 589

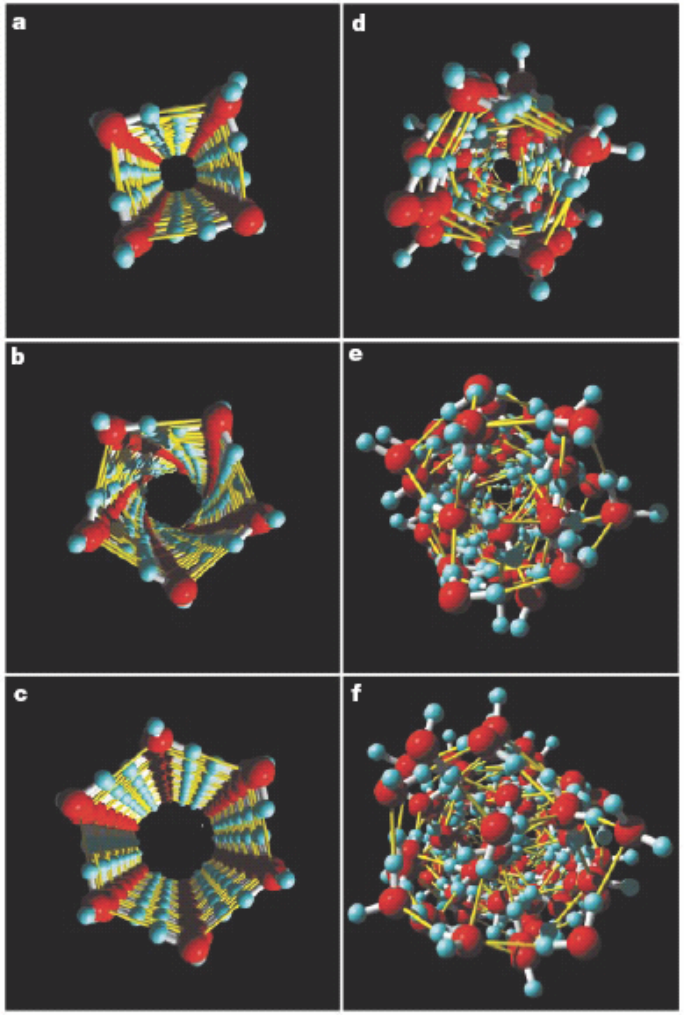


**Figure 2** Snapshots of quenched molecular coordinates. **a**, Square; **b**, pentagonal; **c**, hexagonal ice nanotubes in (14,14), (15,15) and (16,16) SWCNs; **d** to **f**, the corresponding liquid phases. The ice nanotubes were formed on cooling under an axial pressure of 50 MPa in molecular dynamics simulations. The nearest-neighbour distances in both ice nanotube and encapsulated liquid water are fairly constant, about 2.7 to 2.8 Å, and this is in part responsible for the novel phase behaviour.

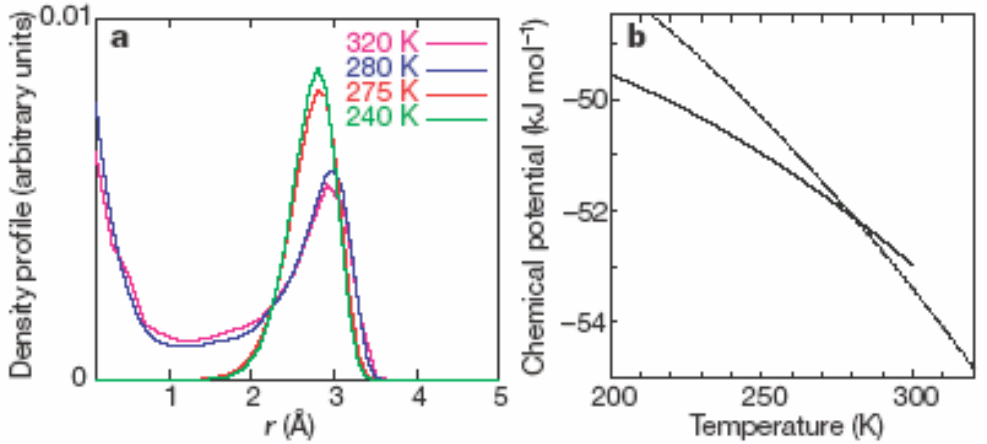


**Figure 3** Properties associated with the first-order phase transition in the (16,16) SWCN at a fixed pressure of 50 MPa. **a**, Radial density profile of confined water at various temperatures. **b**, Chemical potential of liquid water (filled circles and dashed line) and the hexagonal ice nanotube (solid line) against temperature.

"… we found that water can exhibit a first-order freezing transition to hexagonal and heptagonal ice nanotubes, and a continuous phase transformation into solid-like square or pentagonal ice nanotubes."

K. Koga et al., NATURE **412** (2001) 802

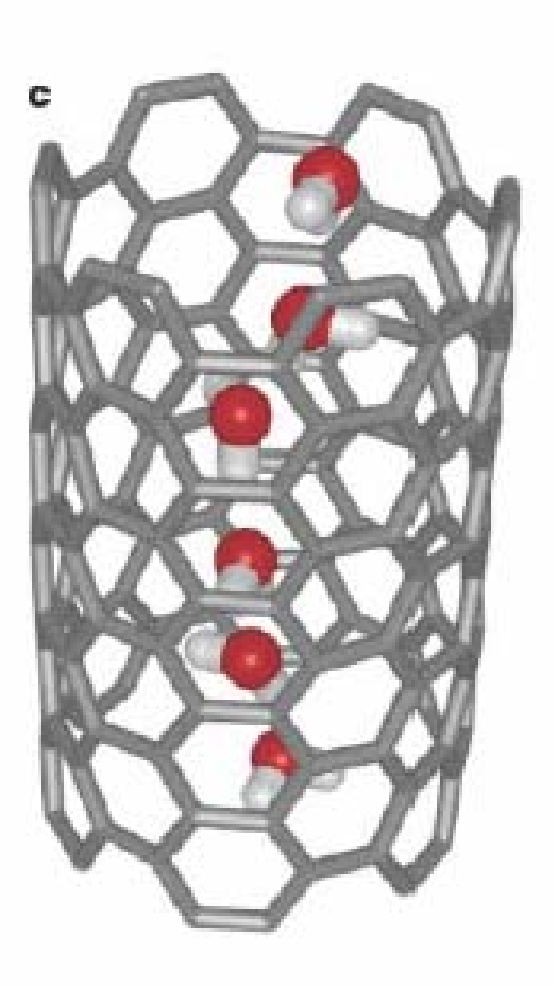


Structure of the hydrogen-bonded water chain inside the nanotube.
"… we observe pulse-like transmission of water through the nanotube."

G. Hummer et al., NATURE **414** (2001) 188

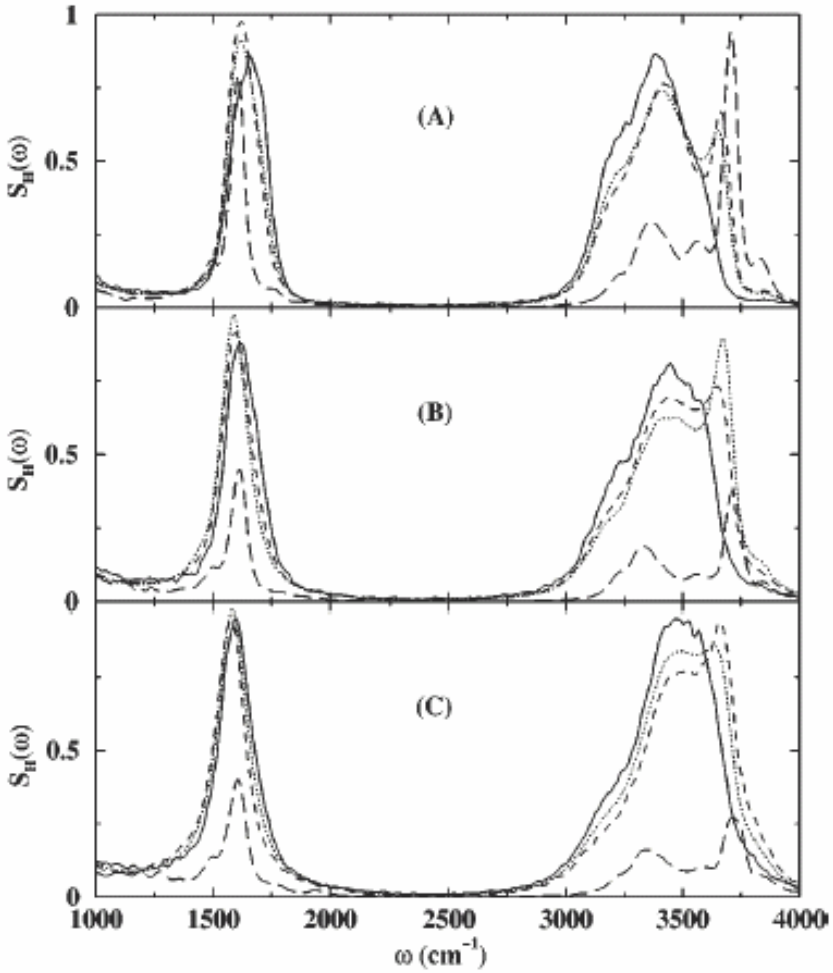


FIG. 5. Hydrogen spectral densities for CN at different temperatures. High frequency range (1000–4000 cm-1). (A) 298 K, (B) 400 K, (C) 500 K. Bulk is represented by full lines at ambient conditions, (6,6) CN are represented by longdashed lines, (8,8) CN are represented by dashed lines, and (10,10) CN are represented by dotted lines. Bulk has been computed at 298, 403, and 523 K.

"The **hydrogen-bond network of constrained water has been revealed to be weaker than the one of bulk water** at all simulated temperatures. … We observed that narrow tubes do not allow complex H-bonded structures and, in many cases, the adsorbed water molecules inside are forming long linear chains. … We have found that diffusion in the *z* direction is clearly faster than the bulk value in all cases.

… One relevant fact is the detection of a high vibrational frequency in the stretching spectral region of all constrained water samples which is absent in the bulk."

J. Martı´ and M.C. Gordillo, Phys. Rev. E 64 (2001) 021504

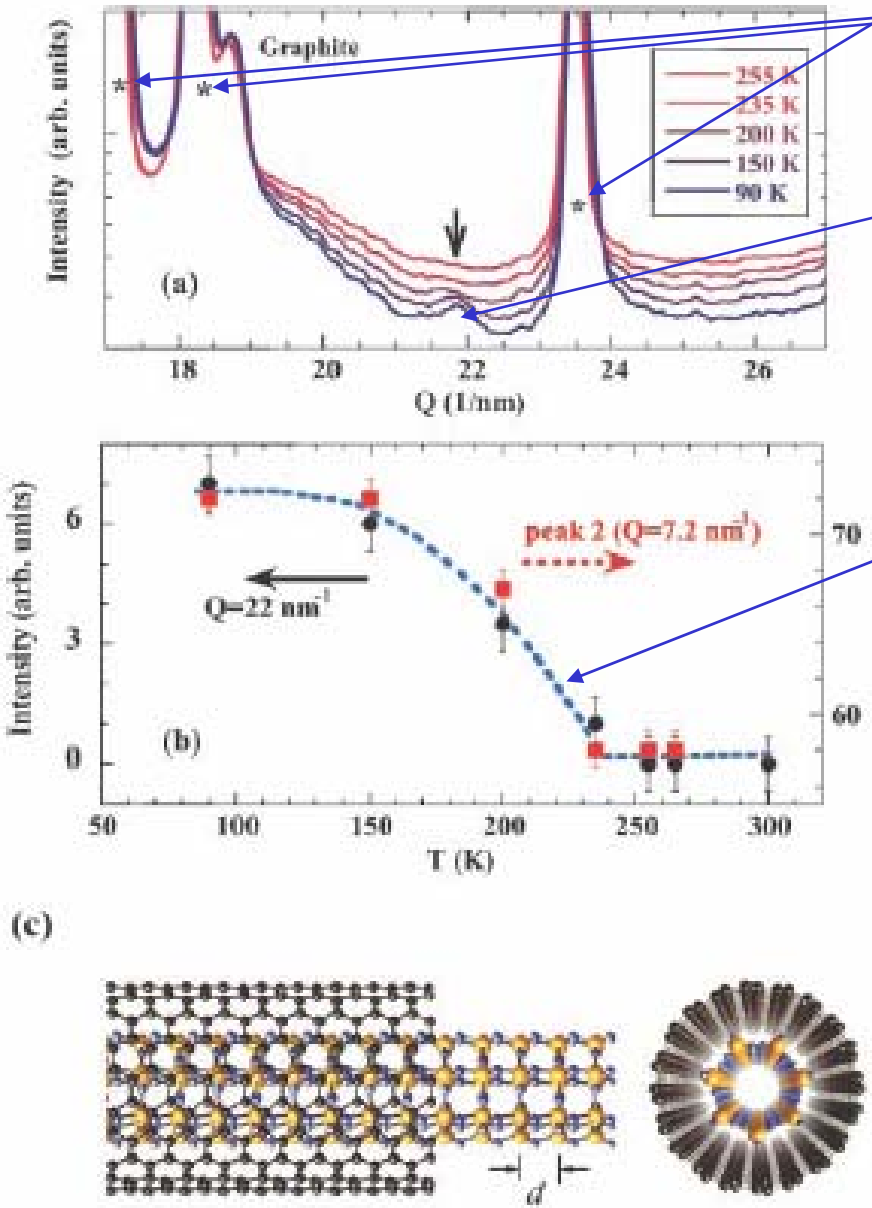


Bulk ice external to the SWNT

Nanotube-ice peak

"Liquid-like water transforms into a new solid form" in nanotube

Fig. 4. (a) Temperature dependence of XRD profiles in water-exposed SWNT bundles. Stars (*) denote peaks due to bulk ice. (b) Temperature dependence of the intensity of the peak around $Q = 22\,\mathrm{nm}^{-1}$ shown by the arrow in (a), along with that of peak 2 at around $Q = 7.2\,\mathrm{nm}^{-1}$. The background intensity due to the presence of a quartz capillary was subtracted. (c) The proposed structure of the ice nanotube inside a SWNT. The estimated $d$-spacing is 0.287 nm at 90 K.

Y. MANIWA et al.,
J. Phys. Soc. Japan **71** ( 2002) 2863

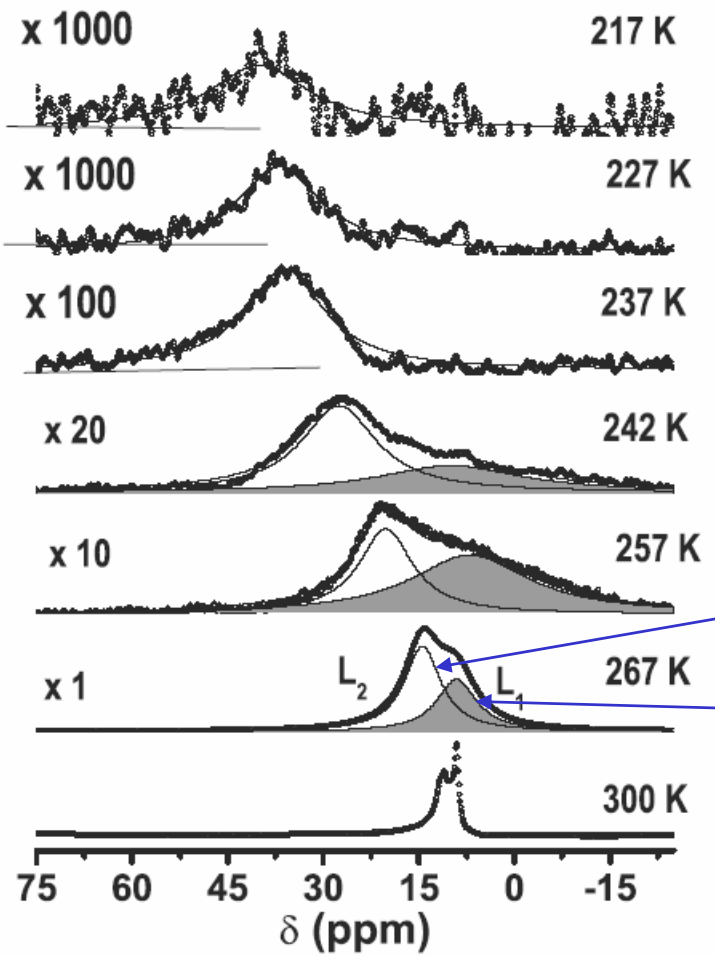


L2 Lorentzian attributed to water near the nanotube wall

L1 Lorentzian attributed to the central water

The disappearance of L1 below ~237 K was interpreted as the transfer of the central water to the water-tube (L2) which subsequently freezes at ~212 K.

Water at nanoscale confined in single-walled carbon nanotubes studied by NMR.

S. Ghosh et al., *Europhys. Lett.* **65** (2004) 678

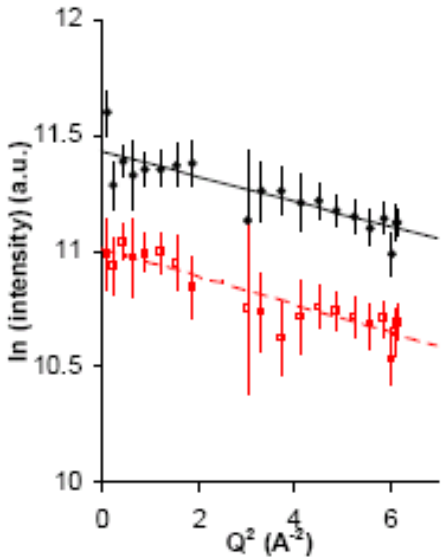


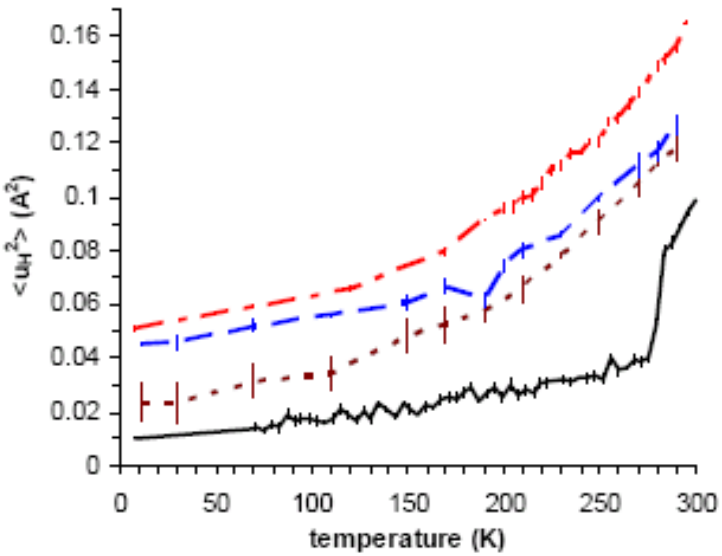


**(Left) Figure 4.** The observed integrated elastic-scattering intensities versus $Q^2$ for the 9.5 wt% water in DWNT at 70 K (full-diamond symbols) and 190 K (empty-square symbols). The expected variation from incoherent scattering of the hydrogen atoms is of the form: exp $(-\langle u_H^2 \rangle Q^2)$. Therefore, $\langle u_H^2 \rangle$ can be obtained from a fit of the ln-intensity vs $Q^2$.

**(Right) Figure 5.** Temperature dependence of $\langle u_H^2 \rangle$ for 9.5 wt% water in DWNT (dashed line) and 5.3 wt % water in SWNT (dotted line), the previous results [2] for 11.3 wt% water in SWNT (dash-dotted line), and bulk water (full line).

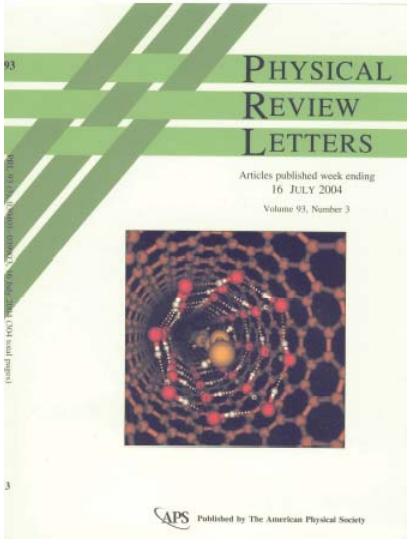


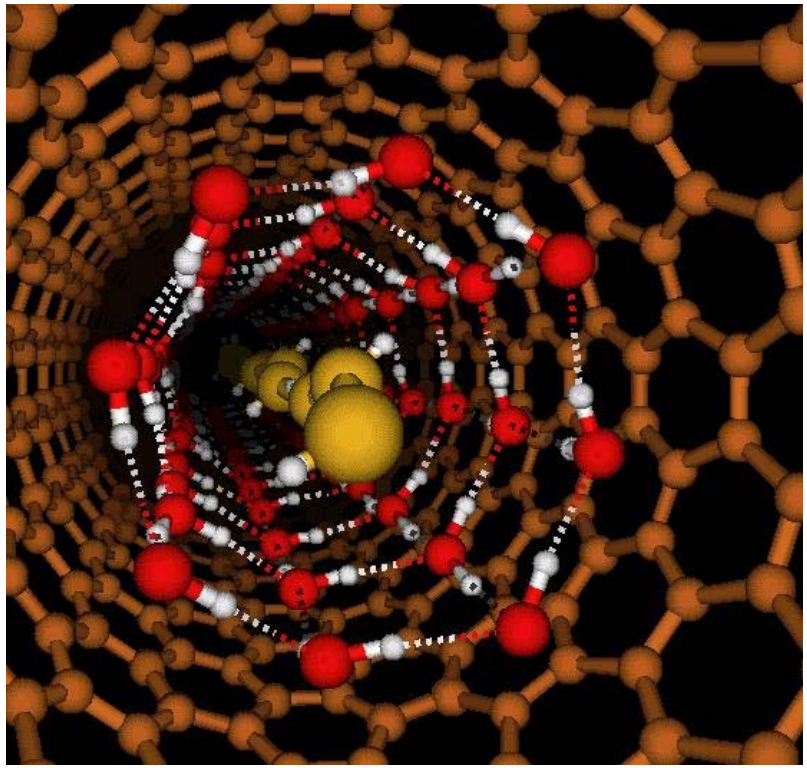

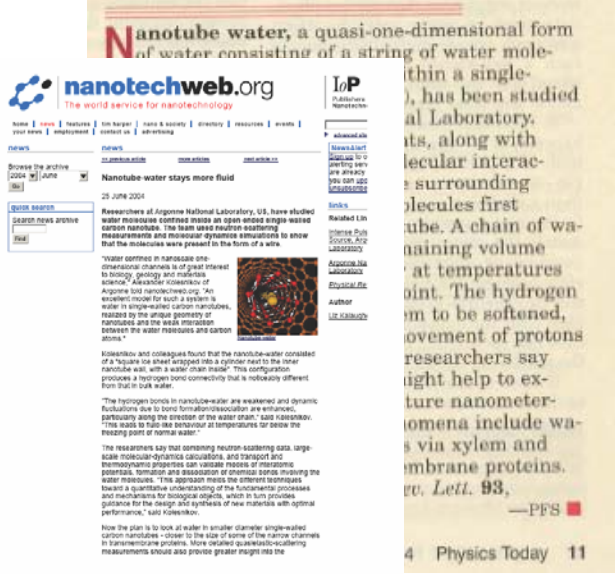






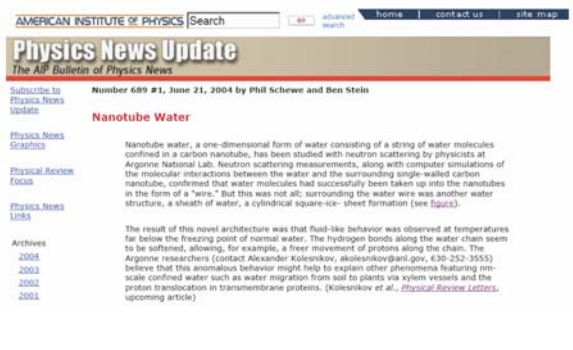




**Proposed structure of nanotube-water. The interior "chain" water molecules have been colored yellow to distinguish them from the exterior "wall" water molecules (colored red).**